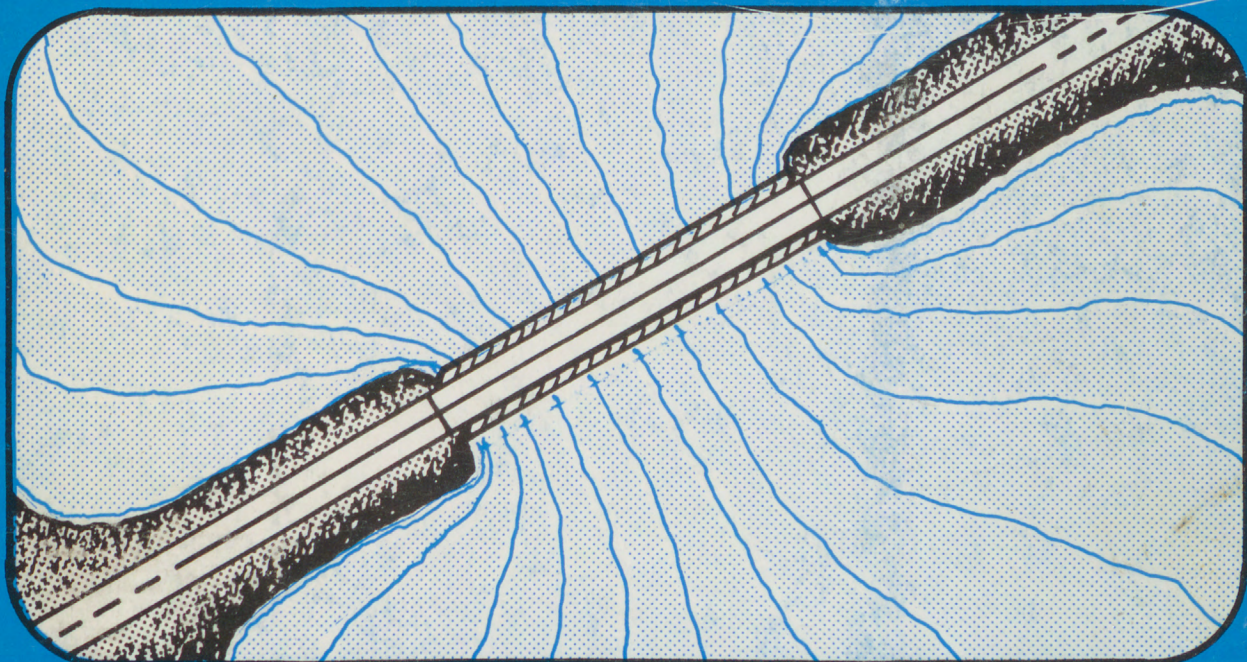


00)  
NRI  
6-76-129

C-2 in process

# *Computation of Backwater And Discharge at Width Constrictions of Heavily Vegetated Flood Plains*



**U.S. GEOLOGICAL SURVEY**  
**Water-Resources Investigation 76-129**

Prepared in Cooperation with the  
Federal Highway Administration and the  
State Highway Departments of  
Mississippi, Alabama, and Louisiana



BIBLIOGRAPHIC DATA SHEET		1. Report No.	2.	3. Recipient's Accession No.
4. Title and Subtitle		5. Report Date June 1975		
COMPUTATION OF BACKWATER AND DISCHARGE AT WIDTH CONSTRICTIONS OF HEAVILY VEGETATED FLOOD PLAINS		6.		
7. Author(s) Verne R. Schneider, James W. Board, B. E. Colson, Fred N. Lee, and Leroy Druffel		8. Performing Organization Rept. No. WRI 76-129		
9. Performing Organization - 12. Sponsoring Organization - 11. Contract/Grant No.				
U.S. Geological Survey 430 Bounds Street Jackson, Mississippi 39206		Mississippi State Highway Dept. P. O. Box 1850 Jackson, Mississippi 39205	HPR-1(4), pt. II, State Study No. 15	
U.S. Geological Survey, WRD 6554 Florida Blvd. Baton Rouge, Louisiana 70806		Louisiana Dept. of Highways P.O. Box 44245, Capital Station Baton Rouge, Louisiana 70804	651H	
U.S. Geological Survey, WRD Room 202 Oil and Gas Board Bldg. University of Alabama University, Alabama 35486		Alabama Highway Dept. Bureau of Research and Development 11 South Union Street Montgomery, Alabama 36104	50-001-009-930-001	
U.S. Geological Survey, WRD Gulf Coast Hydroscience Center Bay St. Louis, Mississippi 39529				
10. Project/Task/Work Unit No. - 13. Type of Report & Period Covered - 14.				
Final report				
15. Supplementary Notes Prepared in cooperation with the U.S. Department of Transportation, Federal Highway Administration.				
16. Abstract Data were collected at 20 single opening bridges for 31 floods. Measured backwater ranged from 0.39 to 3.16 feet (0.12 to 0.96 meters). Backwater computed by the Geological Survey method averaged 29 percent less than the measured and that computed by the Federal Highway Administration method averaged 47 percent less than the measured. Discharge computed by the Geological Survey method averaged 21 percent more than the measured. Analysis of data showed that the flood plain widths and the roughness are larger than those used to develop the standard methods.				
A method to more accurately compute backwater and discharge was developed. The difference between the contracted and natural water-surface profiles computed using standard step-backwater procedures is defined as backwater. The energy loss terms in the step-backwater procedure are computed as the product of the geometric mean of the energy slopes and the flow distance in the reach. An estimate of the average flow distance in the approach reach was derived from potential flow theory. The mean error was 1 percent when using the proposed method for computing backwater and 3 percent for computing discharge.				
17. Key Words and Document Analysis. 17a. Descriptors				
*Backwater, *Flow profiles, *Discharge measurement, *Data collection, Open-channel flow, Manning's equation, Bridges, Gradually varied flow, Energy losses				
17b. Identifiers/Open-Ended Terms Indirect discharge measurement, Bridge backwater data, Floods, Bridge backwater computation				
17c. COSATI Field/Group				
18. Availability Statement No restriction on distribution		19. Security Class (This Report) UNCLASSIFIED	21. No. of Pages 64	
		20. Security Class (This Page) UNCLASSIFIED	22. Price	



## COMPUTATION OF BACKWATER AND DISCHARGE

AT WIDTH CONSTRICtIONS OF

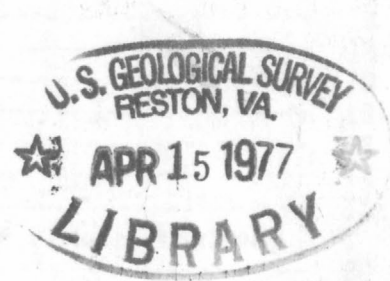
HEAVILY VEGETATED FLOOD PLAINS

By Verne R. Schneider, James W. Board, B. E. Colson,  
Fred N. Lee, and Leroy Druffel

U. S. GEOLOGICAL SURVEY

Water-Resources Investigations 76-129

Prepared in cooperation with the  
Federal Highway Administration and the  
State Highway Departments of  
Mississippi, Alabama, and Louisiana



"The contents of this report reflect the views of the authors who are responsible for the facts and the accuracy of the data presented herein. The contents do not necessarily reflect the official views or policies of the State or the Federal Highway Administration. This report does not constitute a standard, specification or regulation."



February 1977

UNITED STATES DEPARTMENT OF THE INTERIOR

Cecil D. Andrus, Secretary

GEOLOGICAL SURVEY

V. E. McKelvey, Director

---

For additional information write to:

U. S. Geological Survey  
Gulf Coast Hydroscience Center  
National Space Technology Laboratories  
Bay St. Louis, Mississippi 39529

## CONTENTS

	Page
Abstract -----	1
Introduction -----	1
Methods of computing discharge and backwater -----	3
U.S. Geological Survey method-----	3
Discharge -----	3
Backwater -----	5
Federal Highway Administration method-----	6
Backwater -----	6
Data collection-----	7
Peak discharge measurement -----	7
Valley cross sections -----	12
Water-surface elevations -----	12
Bridge geometry-----	13
Manning's roughness coefficient-----	13
Analysis of data -----	13
Computing the natural profile -----	13
Measurement of $h_1^*$ -----	14
Measurement of $h_3^*$ -----	15
Comparison of U.S. Geological Survey and Federal Highway Administration methods-----	20
Energy loss evaluation-----	20
Theoretical analysis -----	24
Energy losses in approach reach-----	25
Energy losses in flow expansion reach-----	33
Proposed method to compute backwater and discharge -----	36
Results-----	37
Conclusions -----	53
Future work-----	54
Example of backwater calculations using proposed method -----	54
References -----	63

## ILLUSTRATIONS

Figure 1. Definition sketch of the variables used in computing backwater and discharge by the Survey method -----	4
2. Graph showing the water-surface elevation on the downstream side of the right embankment, West Fork Amite River near Busy Corner, Mississippi -----	19
3. Graph showing the comparison of measured backwater to that computed by the Survey method -----	21
4. Graph showing the comparison of measured backwater to that computed by the FHWA method -----	22

## ILLUSTRATIONS-continued

		Page
Figure	5. Graph showing the comparison of measured discharge to that computed by the Survey method -----	23
	6. Definition sketch of the variables used in computing backwater and discharge by the proposed method -----	26
	7. Sketch showing the $W$ and $Z$ planes for the Schwartz-Christoffel transformation -----	28
	8. Sketch showing the flow pattern for one-half of a symmetric constriction developed from the potential flow model ( $m = 0.80$ ) -----	28
	9. Graph showing the ratio of the average flow path length in the approach reach and the width of the constricted section as a function of the geometric constriction ratio and the ratio of the distance to the approach cross section and the width of the constriction -----	29
	10. Graph showing the ratio of the distance to the approach section and the width of the constricted section as a function of the geometric constriction ratio -----	34
	11. Graph showing the comparison of measured backwater to that computed by the proposed method -----	40
	12. Graph showing the comparison of measured discharge to that computed by the proposed method -----	44
	13. Graph showing the relation between the percent error in computing backwater by the Survey and proposed methods and the ratio of the measured $L_w$ and proposed $L_w$ -----	45
	14. Graph showing the relation between the percent error in computing discharge by the Survey and proposed methods and the ratio of the measured $L_w$ and proposed $L_w$ -----	46
	15. Diagram showing the plan and approach cross section of Example Creek -----	55

## TABLES

		Page
Table	1. Station location and flood date -----	8
	2. Summary of floods -----	11
	3. Summary of data for computing backwater and discharge by the Survey method -----	16
	4. Summary of data for computing backwater by the FHWA method -----	18

TABLES-continued

	Page
Table 5. Ratio of the average flow path length in the approach reach and the width of the constricted section as a function of the geometric constriction ratio and the ratio of the distance to the approach cross section and the width of the constriction-----	30
6. Ratio of the distance to the approach section and width of the constricted section as a function of the geometric constriction ratio-----	35
7. Summary of data for computing backwater by the proposed method-----	38
8. Comparison of results of computing backwater by the Survey, FHWA, and proposed methods-----	41
9. Summary of data for computing discharge by the proposed method-----	43
10. Summary of data for evaluating the effect of distance to the approach section on the accuracy of the computed backwater and discharge-----	47
11. Summary of data from the verification files for evaluating the effect of distance to the approach section on the accuracy of computed backwater and discharge-----	49
12. Percent errors in computing backwater and discharge as a function of approach section location-----	51
13. Cross-section properties for section 1-----	57

## SYMBOLS AND UNITS

Symbol	Definition	Units
$a_i$	Area of a subsection	$\text{ft}^2$
$A_i$	Area of flow	$\text{ft}^2$
$A_{in}$	Area of flow below the natural water surface elevation	$\text{ft}^2$
$A_p$	Submerged cross-sectional area of piers or piles	$\text{ft}^2$
$A_j$	Projected area of piers normal to flow below the natural water surface elevation	$\text{ft}^2$
$b$	Width of bridge opening	$\text{ft}$
$b_d$	Offset distance for straight dikes	$\text{ft}$
$b_t$	Width of bridge opening at the water surface	$\text{ft}$
$B$	Valley width in the approach reach	$\text{ft}$
$C$	Coefficient of discharge	$\text{ft}$
$C_b$	Backwater ratio, $h_b^*/\Delta h$	
$d$	Subscript denoting a variable measured at the cross section across the upstream toe of the spur dikes	
$D_b$	Differential level ratio, $\frac{h_b^*}{h_b^* + h_3^*}$	
$e$	Eccentricity ratio based on conveyance distribution in approach reach	
$e'$	Eccentricity based on geometry	
$e^c$	$1 - e$	
$E$	Slope of the embankments, horizontal distance/vertical distance	
$g$	Gravitational constant (acceleration)	$\text{ft/s}^2$
$h_i$	Static or piezometric head (stage) above an arbitrary datum at a cross section during constricted flow conditions	$\text{ft}$
$h_{in}$	Static or piezometric head (stage) above an arbitrary datum at a cross section during natural flow conditions	$\text{ft}$
$h_b$	Energy loss caused by the constriction	$\text{ft}$
$h_e$	Energy loss due to flow expansion between sections 3 and 4	$\text{ft}$
$h_{f(i-j)}$	Energy loss due to friction between an upstream and downstream cross section during constricted flow conditions	$\text{ft}$
$h_{f(i-j)n}$	Energy loss due to friction between an upstream and downstream cross section during natural flow conditions	$\text{ft}$
$h_{L(i-j)}$	Total energy loss between an upstream and downstream cross section	$\text{ft}$
$h_i^*$	Total backwater or rise above the natural water surface caused by the constriction at a cross section	$\text{ft}$
$h_b^*$	Backwater computed from the base curve	$\text{ft}$
$i$	Subscript denoting cross-section number	
$(i-j)$	Subscript denoting a variable measured between an upstream (subscript $i$ ) and downstream (subscript $j$ ), cross section	
$k_i$	Conveyance of a subsection	$\text{ft}^3/\text{s}$

Symbol	Definition	Units
$K_i$	Conveyance of cross section	$\text{ft}^3/\text{s}$
$K_c$	Controlling conveyance used for computing flow through the constriction	$\text{ft}^3/\text{s}$
$K_d$	Conveyance of the spur dike cross section	$\text{ft}^3/\text{s}$
$K_q$	Portion of the approach conveyance, $K_1$ , corresponding to the bridge width, $b$	$\text{ft}^3/\text{s}$
$K^*$	Total backwater coefficient	
$L_{av(i-j)}$	Distance between two cross sections	ft
$L_{av(i-j)}$	Average streamline length in the approach reach	ft
$L$	Length of bridge abutment in direction of flow	ft
$L_d$	Length of dikes	ft
$L_w$	Distance from approach section to upstream side of constriction or the toe of the spur dikes when spur dikes are included on the bridge	ft
$L^*$	Distance from point of maximum backwater to water surface on upstream side of roadway embankment measured parallel to center line of stream	ft
$m$	Channel-constriction ratio, $1 - K_q/K_1$	ft
$m'$	Channel-geometric-constriction ratio, $1 - b/B$	
$M$	Bridge opening ratio, $K_q/K_1 = 1 - m$	
$n$	Subscript denoting flow under natural conditions	
$n$	Manning's roughness coefficient	$\text{ft}^{1/6}$
$Q$	Total discharge	$\text{ft}^3/\text{s}$
$S_o$	Slope of channel bottom or natural water-surface profile	
$S_{f(i-j)}$	Friction slope between two cross sections	
$V_i^f$	Mean velocity at a cross section during constricted flow conditions, $Q/A_i$	ft/s
$V_{in}$	Mean velocity at a cross section during natural flow conditions, $Q/A_{in}$	ft/s
$x$	Horizontal distance from the intersection of the abutment and embankment slopes to the location on upstream embankment having the same elevation as the water surface at section 1	ft
$y_i$	Depth of flow at a cross section	ft
$\alpha_i$	Energy coefficient at a cross section	
$\beta_i$	Momentum coefficient at a cross section	
$\delta$	Variable defined by equation 20	
$\varepsilon$	Variable defined by equation 19	
$\Phi$	Angle of skew; acute angle between the plane of the constriction and a line normal to the thread of the stream	

## CONVERSION FACTORS

The conversion factors for the terms used in this report are listed below. The metric equivalents are shown only to the number of significant figures consistent with the values for the English units within the text.

<u>English</u>	<u>Multiply by</u>	<u>Metric</u>
feet (ft)	0.3048	meters (m)
feet (ft)	304.8	millimeter (mm)
cubic feet per second (ft <sup>3</sup> /s)	0.02832	cubic meters per second (m <sup>3</sup> /s)
inches (in)	25.4	millimeters (mm)
miles (mi)	1.609	kilometers (km)
square miles (mi <sup>2</sup> )	2.590	square kilometers (km <sup>2</sup> )

COMPUTATION OF BACKWATER AND DISCHARGE  
AT WIDTH CONSTRICtIONS OF  
HEAVILY VEGETATED FLOOD PLAINS

By Verne R. Schneider, James W. Board, B. E. Colson,  
Fred N. Lee, and Leroy Druffel

ABSTRACT

The U. S. Geological Survey, cooperated with the Federal Highway Administration and the State Highway Departments of Mississippi, Alabama, and Louisiana, to develop a proposed method for computing backwater and discharge at width constrictions of heavily vegetated flood plains. Data were collected at 20 single opening sites for 31 floods. Flood-plain width varied from 4 to 14 times the bridge opening width. The recurrence intervals of peak discharge ranged from a 2-year flood to greater than a 100-year flood, with a median interval of 6 years. Measured backwater ranged from 0.39 to 3.16 feet (0.12 to 0.96 meters). Backwater computed by the present standard Geological Survey method averaged 29 percent less than the measured, and that computed by the currently used Federal Highway Administration method averaged 47 percent less than the measured. Discharge computed by the Survey method averaged 21 percent more than the measured. Analysis of data showed that the flood-plain widths and the Manning's roughness coefficient are larger than those used to develop the standard methods in current use and the accurate computation of backwater and discharge depends on improving the method of computing the energy loss.

With the proposed method for computing backwater and discharge, the contracted and natural water-surface profiles are computed using standard step-backwater procedures. The difference between the profiles is defined as backwater. The energy loss terms in the step-backwater procedure are computed as the geometric mean of the energy slopes and the representative flow distance between the ends of the reach. An estimate of the average flow path was derived from potential flow theory for the approach reach while an empirical method based on the straight-line distance between the bridge and a valley cross section one-bridge-opening width downstream was developed for the flow expansion reach. The mean error using the proposed method for computing backwater was 1 percent. The mean error using the proposed method for computing discharge was 3 percent.

INTRODUCTION

Backwater, caused by the contraction of flow through a width constriction, is the increase in the water-surface elevation above the natural condition. Some width constrictions occur naturally but the most severe, such as highway encroachments, are man-made. Backwater is involved in designing

a bridge including the size of its opening, elevation of the low bridge chord, and size of the inundated flood-plain area.

The change in water-surface elevation induced by flow through existing structures is used to compute the peak discharge of floods. The maximum water-surface elevations upstream and downstream of a constriction after a flood event are determined from high-water marks. The peak discharge is computed from the constriction and flood-plain geometry, flood-plain roughness, and the difference in water-surface elevations upstream and downstream of the constriction.

The U. S. Geological Survey developed methods to compute backwater and discharge based on model studies and verified them with field data. The backwater computation method was reported by Tracy and Carter (1955), and the procedure for applying the method by Cragwall (1958). The method for computing peak discharge at width constrictions was developed by Kindsvater, Carter and Tracy (1953) and Kindsvater and Carter (1955). The procedure is discussed by Matthai (1967).

The FHWA (Federal Highway Administration) developed a method of computing backwater based on model studies and Survey field data. This method was developed by Liu, Bradley and Plate (1957). The computational procedure is described by Bradley (1960, 1970).

Backwater and discharge can be computed with acceptable accuracy with the Survey and FHWA methods for the range of conditions for which they were developed. However, field data reported by B. Neely (written commun., 1966) showed that backwater computed by either method averaged approximately 50 percent less than the measured backwater; the discharge computed by the Survey method with these field data averaged 50 percent more than the measured discharge. Neely's field data were collected at bridge sites on wide, heavily vegetated flood plains with widths varying from 3.5 to 11 times the bridge opening width. Manning's roughness coefficient varied from 0.030 to more than 0.25. The Survey and FHWA methods were developed for flood plains whose widths ranged from 0 to 5 times the bridge opening width and Manning's roughness coefficient up to 0.050; therefore, these methods were not intended for the conditions reported by Neely.

Attempts have been made to develop methods for computing backwater and discharge at width constrictions of heavily vegetated flood plains. Bradley (1970) increased the backwater coefficient for highly-constricted channels based on studies using the field data reported by B. Neely (written commun., 1966). Laursen (1970) suggested that the flow moving laterally toward the bridge accumulates upstream of the bridge and the accumulating flow (accretion rate) causes backwater. Furthermore, heavy vegetation downstream of the bridge causes downstream backwater because of the flow moving back (abstraction rate) onto the flood plain. Laursen combined the accretion and abstraction rates with the flow equations to develop a method to predict backwater. Unfortunately, there is no known method for determining the accretion and abstraction rates from measurable flood-plain variables.

Franques and Yannitell (1974) developed a two-dimensional finite element flow model. The model was applied to one flood on a wide, heavily vegetated flood plain. Although the method is promising, additional work is needed to develop the model to compute backwater for general field applications.

In 1969 the Survey, in cooperation with the FHWA and the Mississippi, Alabama, and Louisiana State Highway Departments, began a 5-year study to collect backwater and discharge data at bridges in wide, heavily vegetated flood plains. The purpose of the study was to develop a method for computing backwater and discharge at width constrictions of heavily vegetated flood plains. Data were collected at 20 single opening bridges. Thirty-one floods were observed where 11 sites had one flood each, 8 sites had two floods each, and 1 site had three floods. Backwater and discharge were computed by the Survey and FHWA methods and were compared with the measured data. The variables affecting the computations were studied to determine the reason for the differences between the computed and measured values. Methods to improve the accuracy of computing backwater and discharge were developed.

## METHODS OF COMPUTING DISCHARGE AND BACKWATER

### U. S. Geological Survey Method

*Discharge.*--Kindsvater and Carter (1955) conducted the analytical and experimental work leading to the development of the Survey method of computing discharge through width constrictions. The discharge relationship is derived from the energy and continuity balance between an approach section and the most contracted section designated sections 1 and 3, respectively, on figure 1,

$$Q = CA_3 \sqrt{2g(\Delta h + a_1 \frac{V_1^2}{2g} - h_f(1 - 3))} \quad (1)$$

where  $Q$  is the total discharge, in  $\text{ft}^3/\text{s}$ ;  $C$  is the discharge coefficient;  $A$  is the flow area below the measured water-surface elevation, in  $\text{ft}^2$ ;  $\Delta h$  is the difference in water-surface elevation between sections 1 and 3, in ft;  $V$  is the mean velocity at a cross section, in  $\text{ft}/\text{s}$ ;  $a$  is the energy coefficient at a cross section; and  $h_f$  is the energy loss due to friction, in ft. A numerical subscript denotes the cross-section number and a compound subscript (for example (1 - 3)) denotes the reach between two cross sections.

Laboratory investigations were conducted to define the discharge coefficients for four typical abutment geometries. The procedures for selecting the discharge coefficients are discussed by Matthai (1967).

The energy loss due to friction is the product of the geometric mean of the energy slopes at the end cross sections of the reach and the distance between the sections. For example, where spur dikes are included on the bridge, the energy loss due to friction is

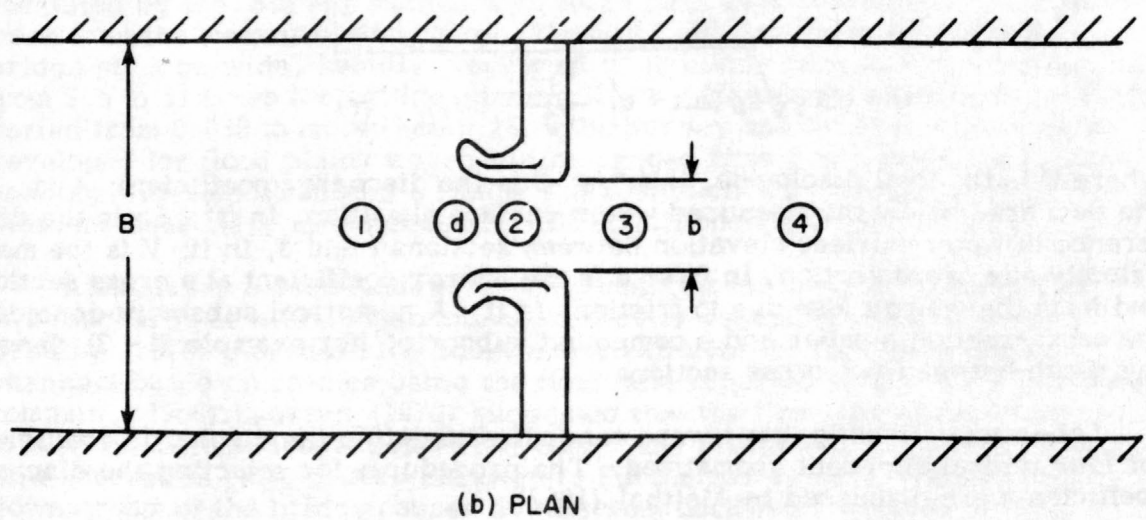
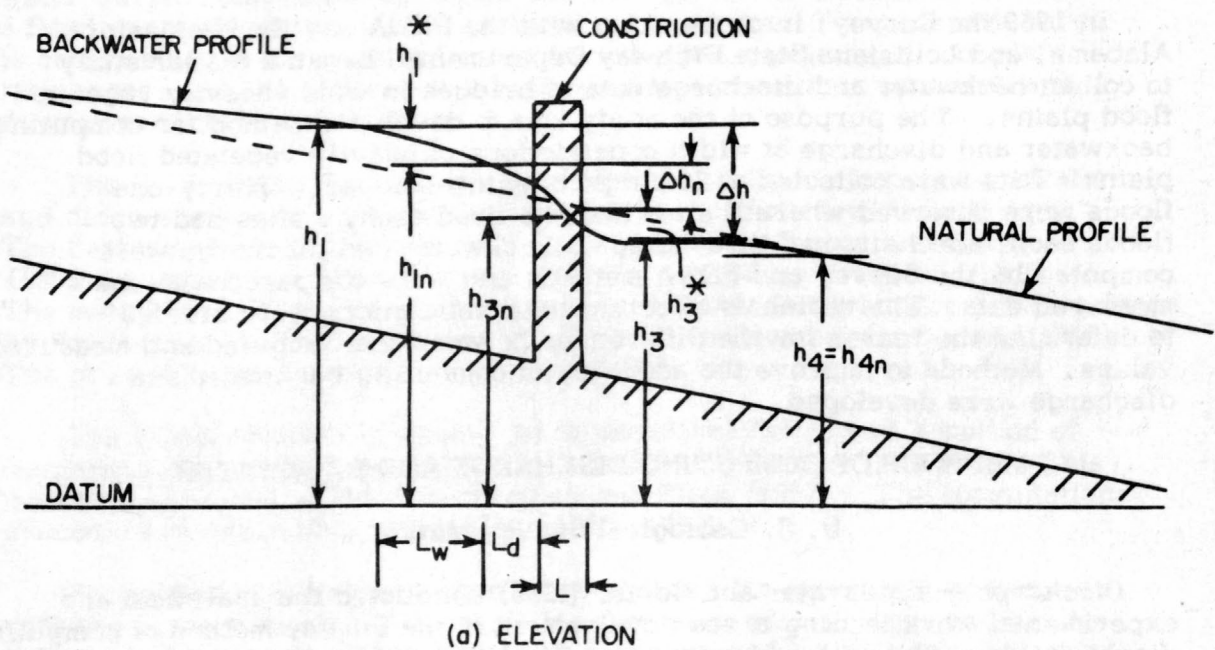


Figure 1.--Definition sketch of the variables used in computing backwater and discharge by the Survey method.

$$h_{f(1-3)} = \frac{L_w Q^2}{K_1 K_q} + \frac{L_d Q^2}{K_d K_3} + \frac{L Q^2}{K_3^2} \quad (2)$$

where  $L_w$  is the distance from the approach section to the upstream side of the constriction or the toe of the spur dikes where they are present, in ft;  $K$  is the conveyance at a cross section, in  $\text{ft}^3/\text{s}$ ;  $K_q$  is that portion of the approach conveyance,  $K_1$ , in  $\text{ft}^3/\text{s}$ , corresponding to the bridge width,  $b$ , in ft;  $L_d$  is the length of the spur dikes, in ft;  $K_d$  is the conveyance of the cross section at the toe of the spur dikes, in  $\text{ft}^3/\text{s}$ ; and  $L$  is the length of the bridge abutment in the direction of flow, in ft.

**Backwater.**--Tracy and Carter (1955) defined backwater,  $h_1^*$ , as one component of the fall,  $\Delta h$ , between sections 1 and 3 as illustrated in figure 1. The fall,  $\Delta h$  was resolved into three components,

$$\Delta h = h_1^* + h_3^* + h_{f(1-3)} n \quad (3)$$

where  $h_1^*$  is the increase in the water-surface elevation at section 1 above the natural condition caused by the contraction of the flow through the width constriction, in ft;  $h_3^*$  is the backwater at section 3, in ft; and  $n$  is a subscript denoting flow under natural conditions.

When equation 3 was divided by  $\Delta h$ ,

$$\frac{h_1^*}{\Delta h} = 1 - \frac{h_3^*}{\Delta h} - \frac{h_{f(1-3)} n}{\Delta h} \quad (4)$$

The ratio,  $\frac{h_1^*}{\Delta h}$ , was defined as the backwater ratio,  $C_b$ . Equation 1 was solved for  $\Delta h$  and  $V_3 = Q/A_3$  was substituted from continuity,

$$h_1^* = C_b \left( \frac{V_3^2}{2gC^2} + h_{f(1-3)} - \alpha_1 \frac{V_1^2}{2g} \right) \quad (5)$$

The backwater ratio is a function of the channel-constriction ratio, Manning's  $n$  value, and the constriction geometry. Equation 5 was substituted into equation 4 and  $h_3^*$  was solved for

$$h_3^* = (1 - C_b) \left( \frac{V_3^2}{2gC^2} + h_{f(1-3)} - \alpha_1 \frac{V_1^2}{2g} \right) - h_{f(1-3)} n. \quad (6)$$

The procedures for computing backwater by the Survey method are contained in Cragwall (1958).

## Federal Highway Administration Method

*Backwater.*--The FHWA method of computing backwater was developed by Lui, Bradley and Plate (1957). The energy relationship between the approach section 1 assumed to be located at the point of maximum backwater and section 4, the point downstream from the bridge where the natural stage is re-established, is

$$S_o L_{1-4} + y_1 + \alpha_1 \frac{V_1^2}{2g} = y_4 + \alpha_4 \frac{V_4^2}{2g} + h_L (1-4) \quad (7)$$

where  $h_L$  is the total energy loss, in ft;  $y$  is the depth of flow at a cross section, in ft; and  $S_o$  is the channel slope.

In the unconstricted channel, the energy loss due to friction is balanced by the channel fall,  $S_o L_{1-4}$ . The total energy loss in the constricted channel,  $h_L (1-4)$ , is assumed to be the sum of the friction loss for the unconstricted channel,  $S_o L_{1-4}$ , and an excess loss due to the constriction,  $h_b$ . The excess loss is defined as the product of an energy loss coefficient,  $K^*$  (later called the total backwater coefficient) and a known velocity head

$$h_b = K^* \alpha_2 \frac{V_{2n}^2}{2g} \quad (8)$$

where  $V_{2n}$  is the mean velocity at section 2 under natural conditions. The numerical subscript refers to the section number and  $n$  refers to natural conditions. Backwater was defined as  $h_1^* = y_1 - y_4$ , equation 8 was substituted into equation 7 and the continuity equation applied

$$h_1^* = K^* \alpha_2 \frac{V_{2n}^2}{2g} + \alpha_1 \left[ \left( \frac{A_{2n}}{A_{4n}} \right)^2 - \left( \frac{A_{2n}}{A_1} \right)^2 \right] \frac{V_{2n}^2}{2g} \quad (9)$$

The specific location of section 4 is not defined. The approach section location,  $L^*$ , is an empirical function of the flow depth under the bridge, the width of the constriction, and the eccentricity. The total backwater coefficient,  $K^*$ , is the sum of the backwater coefficient for the base abutment shape and incremental backwater coefficients for skew, piers, and eccentricity.

Values of  $h_3^*$  are computed by the relationship,

$$h_3^* = h_b^* \left( \frac{1}{D_b} - 1 \right) \quad (10)$$

where  $h_b^*$  is the backwater computed from equation 9 for a normal crossing, without piers, eccentricity, or skew, and  $D_b$  is the differential level ratio.

Lui, Bradley and Plate (1957) conducted extensive laboratory experiments to define the coefficients,  $K^*$  and  $D_b$ , and the distance to maximum backwater,  $L^*$ . The procedure for applying the FHWA method is described by Bradley (1970).

## DATA COLLECTION

Field data were collected using the procedure outlined by Benson and Dalrymple (1967) and Matthai (1967). Data include peak discharge, valley cross sections, water-surface elevations, bridge geometry, and Manning's roughness coefficient,  $n$ . High-water-mark elevations, valley cross-section ground elevations, embankment water-surface elevations, highway profile, and bridge geometry were surveyed using reciprocal leveling techniques. High-water-mark elevations were measured accurate to 0.01 ft (3 mm) and ground-surface elevations and highway profile to 0.1 ft (30 mm). The location of each station and flood date are contained in table 1 and a summary of floods in table 2.

The total data set as reduced and assembled generally includes the following:

1. Summary
  - A. Location of site
  - B. Description of site
  - C. Description of flood
  - D. Description of discharge measurement
  - E. Field survey
  - F. Computations
  - G. Results of computations
  - H. Datum
2. Topographic map
3. Aerial photographs
4. Highway plans
5. Flood-frequency curve
6. Stage-discharge relation
7. Discharge measurement notes
8. Velocity distribution and measuring section diagram
9. Plan of roadway crossing and location of high-water marks
10. Bridge geometry
11. List of high-water marks
12. Water-surface profile along highway embankments
13. Valley cross sections
14. Flood profiles
15. Field notes
16. Computer printouts
17. Stereo slides documenting flood-plain roughness

### Peak Discharge Measurement

Peak discharge was measured by current meter at the flood peak or obtained from stage-discharge relations. The stage-discharge relations were extrapolated several feet at some sites. Available data on the volume of run-off and the duration

Table 1.--Station location and flood date

Flood number	Station number	Station name and location	Date of flood peak
1	02362740	Pea Creek near Louisville, Ala. Lat $31^{\circ}49'08''$ , long $85^{\circ}34'08''$ , in NW $\frac{1}{4}$ sec. 29, T. 10 N., R. 25 E., Barbour County, at bridge on county road 27, 2.9 mi north of Louisville, Ala.	12-21-72
2	02362780	Buckhorn Creek near Shiloh, Ala. Lat $31^{\circ}46'38''$ , long $85^{\circ}43'07''$ , in NW $\frac{1}{4}$ sec. 11, T. 9 N., R. 23 E., Pike County, at bridge on State Highway 130, 1.8 mi east of Shiloh, Ala.	03-02-72
3	02362780	Buckhorn Creek near Shiloh, Ala.	12-21-72
4	02363260	Whitewater Creek near Tarentum, Ala. Lat $31^{\circ}38'11''$ , long $85^{\circ}55'22''$ , in SW $\frac{1}{4}$ sec. 26, T. 8 N., R. 21 E., Pike County, at bridge on county road, 2.7 mi west of Tarentum, Ala.	03-02-72
5	02363330	Big Creek near Spring Hill, Ala. Lat $31^{\circ}40'41''$ , long $85^{\circ}59'39''$ , in SE $\frac{1}{4}$ sec. 12, T. 8 N., R. 20 E., Pike County, at bridge on county road 6, 2.1 mi west of Spring Hill, Ala.	12-06-72
6	02367400	Yellow River near Sanford, Ala. Lat $31^{\circ}19'02''$ , long $86^{\circ}21'21''$ , in NW $\frac{1}{4}$ sec. 16, T. 4 N., R. 17 E., Covington County, at bridge on county road 42, 2.5 mi northeast of Sanford, Ala.	12-21-72
7	02367400	Yellow River near Sanford, Ala.	03-12-73
8	02367490	Poley Creek near Sanford, Ala. Lat $31^{\circ}19'34''$ , long $86^{\circ}18'01''$ , in SE $\frac{1}{4}$ sec. 12, T. 4 N., R. 17 E., Covington County, at bridge on county road, 5.6 mi east of Sanford, Ala.	12-21-72
9	02367490	Poley Creek near Sanford, Ala.	03-12-73
10	02472546	Okatoma Creek near Magee, Miss. Lat $31^{\circ}53'03''$ , long $89^{\circ}41'57''$ , in NE $\frac{1}{4}$ sec. 32, T. 1 N., R. 17 W., Choctaw meridian, on county highway, 2.0 mi east of Mississippi Highway 541 in Magee, and 1.5 mi upstream of Mississippi Highway 28, Simpson County	04-12-74
11	02472550	Okatoma Creek near Magee, Miss. Lat $31^{\circ}51'52''$ , long $89^{\circ}41'25''$ , in sec. 3, T. 10 N., R. 17 W., St. Stephens meridian, on Mississippi Highway 28, 1.4 mi east of old U.S. Highway 49 in Magee, Simpson County.	04-12-74

Table 1.--Continued

Flood number	Station number	Station name and location	Date of flood peak
12	02473460	Tallahala Creek at Waldrup, Miss. Lat $31^{\circ}57'30''$ , long $89^{\circ}06'50''$ , in SW $\frac{1}{4}$ sec. 31, T. 2 N., R. 12 E., Choctaw meridian, on Mississippi Highway 528, 0.8 mi east of Waldrup, Jasper County.	04-14-69
13	02473460	Tallahala Creek at Waldrup, Miss.	04-13-74
14	02474776	Thompson Creek near Clara, Miss. Lat $31^{\circ}33'26''$ , long $88^{\circ}51'33''$ , on sec. line between secs. 23 and 24, T. 7 N., R. 9 W., St. Stephens meridian, at U.S. Forest Service Highway, 2 mi downstream from mouth of Little Thompson Creek and 9.5 mi west of Clara, Wayne County.	03-03-71
15	02484300	Yockanookany River near Thomastown, Miss. Lat $32^{\circ}51'10''$ , long $89^{\circ}39'04''$ , in NE $\frac{1}{4}$ sec. 35, T. 12 N., R. 6 E., Choctaw meridian, on Mississippi Highway 429, 0.8 mi east of Natchez Trace Parkway and 1.3 mi southeast of Thomastown, Leake County.	04-12-69
16	02484300	Yockanookany River near Thomastown, Miss.	01-02-70
17	02490357	Bogue Chitto at Johnston Station, Miss. Lat $31^{\circ}20'09''$ , long $90^{\circ}26'07''$ in SE $\frac{1}{4}$ sec. 6, T. 4 N., R. 8 E., Washington meridian, on county highway, 4.2 mi northeast of Summit, 3.7 mi upstream from Mississippi Highway 570, and 1 mi southeast of Johnston Station, Pike County.	12-07-71
18	02490357	Bogue Chitto at Johnston Station, Miss.	03-25-73
19	02490357	Bogue Chitto at Johnston Station, Miss.	04-13-74
20	02490360	Bogue Chitto near Summit, Miss. Lat $31^{\circ}17'50''$ , long $90^{\circ}23'41''$ , in SW $\frac{1}{4}$ sec. 22, T. 4 N., R. 8 E., Washington meridian, on Mississippi Highway 570, 4.8 mi east of U.S. Highway 51 in Summit, Pike County.	12-07-71
21	02490360	Bogue Chitto near Summit, Miss.	04-13-74
22	07275700	Coldwater River near Red Banks, Miss. Lat $34^{\circ}53'35''$ , long $89^{\circ}33'30''$ , on section line between sec. 19, T. 2 S., R. 3 W., and sec. 24, T. 2 S., R. 4 W., Chickasaw meridian, on county highway 4.7 mi north of U.S. Highway 78 at Red Banks, Marshall County.	12-30-69
23	07275700	Coldwater River near Red Banks, Miss.	02-22-71

Table 1.--Continued

Flood number	Station number	Station name and location	Date of flood peak
24	07364735	Little Bayou deLoutre near Truxno, La. Lat $32^{\circ}56'54''$ , long $92^{\circ}25'36''$ , in SW $\frac{1}{4}$ sec. 25, T. 23 N., R. 1 W., Louisiana meridian, at bridge on parish road 1.3 mi west of Truxno, La., Union Parish.	04-22-74
25	07366353	Cypress Creek near Downsville, La. Lat $32^{\circ}39'22''$ , long $92^{\circ}26'35''$ , in SW $\frac{1}{4}$ sec. 2, T. 19 N., R. 1 W., Louisiana meridian, at bridge on State Highway 151, 2.7 mi NW of Downsville, La., Union Parish.	02-21-74
26	07373210	Flagon Bayou near Libuse, La. Lat $31^{\circ}23'00''$ , long $92^{\circ}17'48''$ , in NE $\frac{1}{4}$ S $\frac{1}{2}$ lot 38, T. 5 N., R. 2 E., at bridge on State Highway 116, at Esler Field Airport, 8.8 mi N.E. of Pineville, La., Grant Parish.	12-07-71
27	07373800	Alexander Creek near St. Francisville, La. Lat $30^{\circ}47'36''$ , long $91^{\circ}22'03''$ , between lots 51 and 52, T. 3 S., R. 3 W. at bridge on State Highway 10, 1.7 mi N.E. of St. Francisville, La., West Feliciana Parish.	09-16-71
28	07373800	Alexander Creek near St. Francisville, La.	12-07-71
29	07376692	West Fork Amite River near Busy Corner, Miss. Lat $31^{\circ}14'23''$ , long $90^{\circ}49'24''$ , in NE $\frac{1}{4}$ sec. 7, T. 3 N., R. 4 E., Washington meridian, on Mississippi Highway 567, 6.5 mi north of Liberty, Amite County.	12-06-71
30	07376692	West Fork Amite River near Busy Corner, Miss.	03-25-73
31	08014200	Tenmile Creek near Elizabeth, La. Lat $30^{\circ}50'11''$ , long $92^{\circ}52'26''$ , in NW $\frac{1}{4}$ SW $\frac{1}{4}$ sec. 34, T. 2 S., R. 5 W., at bridge on State Highway 112, 5.3 mi SW of Elizabeth, La., Allen Parish.	12-07-71

Table 2.--Summary of floods

Flood number	Drainage area (square miles)	Flood Peak discharge (cubic feet per second)	Recurrence interval (years)	Length of reach (feet)	Average flood plain width (feet)	Average flood plain flow depth (feet)	Channel slope (feet per mile)	Dike Type	Manning's roughness coefficient
1	58.0	1,780	2	7,000	1,200	2.7	6.9	--	0.14
2	42.2	2,250	6	7,400	1,000	4.1	5.8	--	0.13
3	42.2	4,150	28	7,400	1,070	5.3	5.8	--	0.15
4	105	5,600	6	10,250	1,870	4.3	5.3	Elliptical	0.13
5	26.7	1,550	3	2,600	840	2.8	8.4	--	0.13 -0.20
6	28.2	2,000	2	5,700	920	3.6	7.4	--	0.14
7	28.2	6,600	30	5,700	1,140	5.9	7.8	--	0.13
8	28.3	1,900	2	4,400	1,000	2.9	8.4	--	0.11
9	28.3	4,600	11	4,400	1,090	5.0	8.4	--	0.13
10	24	12,100	>100	10,500	1,500	6.9	7.5	--	0.04 -0.18
11	38	16,100	>100	10,000	1,700	7.8	5.0	--	0.04 -0.18
12	105	12,500	32	24,000	3,000	5.5	4.4	Straight	0.06 -0.25
13	105	17,500	>100	24,000	3,000	6.0	4.4	Straight	0.06 -0.25
14	87.7	3,800	2	3,500	3,500	2.5	2.6	Straight	0.20
15	410	10,200	4	37,000	4,600	4.3	2.5	Elliptical	0.06 -0.14
16	410	8,100	2	37,000	4,600	4.3	2.5	Elliptical	0.06 -0.14
17	208	25,000	18	21,000	5,000	4.7	5.5	--	0.065 -0.25
18	208	31,500	42	21,000	5,000	5.5	5.5	--	0.065 -0.25
19	208	31,000	40	21,000	5,000	5.5	5.5	--	0.065 -0.25
20	255	25,600	15	18,000	3,500	7.0	8.0	Elliptical	0.06 -0.15
21	255	29,500	25	18,000	3,500	7.7	8.0	Elliptical	0.06 -0.15
22	104	3,500	2	33,000	2,300	2.0	6.3	--	0.11
23	104	4,900	3	33,000	2,300	2.0	6.3	--	0.11
24	45.2	4,200	35	5,300	1,600	3.0	5.0	--	0.09 -0.20
25	15.3	1,500	4	4,500	800	2.5	8.0	--	0.10 -0.21
26	73	4,740	5	15,000	1,700	3.0	6.0	--	0.06 -0.17
27	23.9	5,500	2.5	6,000	800	3.0	10.0	--	0.05 -0.20
28	23.9	9,500	5	6,000	800	4.0	10.0	--	0.04 -0.18
29	65	14,200	> 100	16,000	2,400	6.8	5.5	Elliptical	0.06 -0.15
30	65	17,000	> 100	16,000	2,400	7.0	5.5	Elliptical	0.06 -0.15
31	94.2	6,400	6	13,000	2,500	3.0	4.0	--	0.08 -0.20

of the peak indicated that steady flow existed throughout the reach during the peak at most sites. When necessary, flow over the highway embankment was computed using the procedure described by Hulsing (1967). In these cases the amount of flow over the highway embankment was small compared to the total discharge.

#### Valley Cross Sections

In general, eight valley cross sections were selected for a distance of approximately four valley widths upstream and downstream of the highway embankment. In addition, an approach cross section was surveyed approximately one bridge-opening width upstream from the constriction. Additional cross sections were selected as required to define road fills, pipeline crossings and other features affecting the flood profile.

Locations for the valley cross sections were selected by inspection of quadrangle maps. The cross sections were drawn on the map at approximately valley-width intervals and were alined perpendicular to the assumed direction of flow. Identifiable landmarks were used to locate the cross sections in the field, where they were oriented to the correct azimuth by compass. In most cases, high-water marks were selected along the cross sections. The survey datum was established at the bridge. A base line was surveyed from the highway to establish horizontal and vertical control for the cross sections.

The technique for selecting cross sections was improved for several sites in the latter part of the project. A base line was surveyed along each edge of the flood plain, and high-water marks were selected along these lines. A plan view of the reach was drawn showing the base lines, the location and elevation of the high-water marks, and other features affecting the flood profile. The cross sections were located on the plan view at approximately valley width intervals and were alined to intersect the base lines at equal water-surface elevations. Cross sections selected in this manner are assumed to be perpendicular to the flow direction. The cross sections were located in the field using the base lines and were alined to the correct azimuth by compass.

Selecting the location of cross sections based on available high-water information improved the quality of the data. The need to correct for transverse sloping water-surface profiles because of cross section misalignment was eliminated. An adequate number of high-water marks was obtained to provide detailed definition of the flood profile. Undefined valley expansions and contractions and other features affecting the profile which postdated the available quadrangle maps and aerial photography were identified including the location of abandoned roads, railroads, pipelines, power lines, and flood-plain development such as timber harvesting, land clearing and oil drilling. In all cases, the resulting data were easier to interpret.

#### Water-Surface Elevation

Water-surface elevations were determined by high-water marks recovered along the cross sections and base lines. They were marked along the upstream and downstream sides of the embankment during the peak discharge measurement. Additional high-water marks were selected at random locations upstream and downstream of the bridge to describe the lines of constant water-surface elevation in the approach and flow-expansion reaches.

## Bridge Geometry

Bridge geometry data, collected according to the procedures discussed by Matthai (1967), included abutment slope, bridge cross section, and pier and spur dike geometry and location.

### Manning's Roughness Coefficient

An attempt was made to field-select Manning's roughness coefficient,  $n$ . Selection is usually based on experience obtained by computing water-surface profiles in channels where peak discharge and water-surface elevations are known ( $n$ -verification studies) and by studying stereo slides that document features affecting the magnitude of  $n$ . Although  $n$  was selected by experienced personnel and, at most sites, by the same individual for consistency, neither published  $n$ -verification studies nor stereo slides were available for comparative purposes. Therefore, the field-selected  $n$ 's were verified using the measured discharge and the recovered water-surface profile downstream of the bridge. Cross sections were subdivided for major changes in geometry and roughness which persisted throughout the reach and  $n$  selected for each subdivision. For example, when the reach included an open-field which extended approximately one-half the distance upstream and downstream to the next cross sections, the reach was subdivided and  $n$  selected for the open-field condition. Composite  $n$ -values were selected where frequent roughness changes occurred that did not affect the entire reach.

## ANALYSIS OF DATA

Backwater is the difference between the measured contracted and the natural water-surface elevation. The natural (unconstricted) profile is computed using standard-step-backwater techniques (Chow, 1959). The backwater was measured at the location recommended by Survey and FHWA methods. Backwater was computed using the Survey and FHWA methods and discharge was computed using the Survey method. The measured and computed backwater and discharge were compared.

The total energy losses were computed from the field data and by the Survey method for each site and compared to determine the accuracy of the computation method; that is, the product of the geometric mean friction slope and the straight line distance between sections.

### Computing the Natural Profile

The natural water-surface profile was computed by step-backwater methods. Since a natural profile had not been measured prior to construction of the bridge, considerable judgment was exercised in determining the most likely natural profile. Although the flow was not uniform in the strictest sense, for practical purposes, the properties of uniform steady flow can be applied to the overall reach.

In the step-backwater procedure, measured peak discharge, cross-section geometry, and  $n$ -values were used to compute the water-surface profile. The water-surface elevation at the initial section (the most downstream section) was used as the starting elevation. The field selected  $n$ -values were adjusted until the computed profile matched the measured natural water-surface profile downstream and at points three or more valley widths upstream of the bridge, within a reasonable tolerance. The tolerance allowed depended primarily on the variability of the high-water-mark elevations. The computed profile was examined to insure that it properly reflected the known physical features of the flood plain and that it adequately considered all of the uniform flow characteristics. All cross sections whose geometry might have been affected by the bridge construction, such as sections along the rights-of-way and bridge sections, were omitted from the computation.

The following characteristics were considered when computing the natural profile:

1. The natural water-surface profile should, in general, be parallel to the mean flood-plain profile. In most instances, because the main channel area was small, the mean flood-plain elevation was computed by subtracting the hydraulic depth (cross-section area divided by top width) from the water-surface elevation. Otherwise, judgment was used in determining a representative flood-plain elevation.
2. The water-surface profile responds in predictable ways to natural constrictions and expansions, changes in roughness, and other flood-plain land use.
3. The  $n$ -values should be consistent within and among the sites.
4. In most cases, the recovered profile downstream of the bridge was the natural profile, therefore,  $n$ -values that were representative of the site could be computed.
5. Backwater effects observed in the field usually extended no more than two to three valley widths upstream of the bridge so the water-surface elevation beyond that point was assumed to be at the natural elevation.

#### Measurement of $h_1^*$

In the Survey method, backwater,  $h_1^*$  is defined as the difference between the contracted water-surface elevation and the computed natural profile at the approach section, one bridge-opening width upstream. Measured  $h_1^*$  was obtained by subtracting the computed natural water-surface elevation from the measured contracted elevation at the approach section. The field data showed that the measured water-surface elevation in the approach reach along the edge-of-water was nearly constant, that is ponded conditions existed at these sites.

In the FHWA method, maximum backwater is located a distance,  $L^*$ , upstream of the constriction on the centerline of the bridge opening. This distance is an empirical function of the mean depth of flow under the bridge (at section 3) below normal stage,  $\frac{A}{b} 2n$ , the total fall through the bridge ( $h_1 - h_3$ ), and the eccentricity. The contracted water-surface elevation was not measured at  $L^*$  in the field. However, the FHWA method assumes that for distances along the upstream side of the embankment greater than  $L^*$ , the contracted water-surface elevation is equal to that at  $L^*$ . Therefore,  $h_1^*$  was measured as the difference between the water-surface elevation along the upstream side of the embankment a distance  $L^*$  from the bridge centerline and the computed natural water-surface elevation at the distance,  $L^*$ , upstream of the constriction. Tables 3 and 4 contain the values of  $h_1^*$  for each site.

#### Measurements of $h_3^*$

The difference between the contracted water-surface elevation and the computed natural profile at section 3 is defined as  $h_3^*$ . The measurement of  $h_3^*$  is complicated by the flow expansion process downstream of the bridge which is different from that observed by Kindsvater and Carter (1955) and Lui, Bradley, and Plate (1957). In those studies, the flow separated from the abutment and formed a large eddy on the downstream side of the constriction; the flow reattached at the edge of the flood plain downstream. The water-surface elevation of the stream at the vena contracta was approximately equal to the elevation along the embankment and was always below the natural water-surface elevation. Therefore, the water-surface elevation along the downstream side of the embankment was used as reference elevation for computing backwater and discharge by the Survey and FHWA methods.

In this study, the flow was observed to separate from the abutment but reattached on the embankment a short distance away. The large eddy observed previously did not occur at these sites. The vena contracta is located near section 3. The water flows outward in all directions to the edge of the valley. The water-surface elevation along the embankment slopes downward toward the flood-plain edge. Field data from the West Fork Amite River, Mississippi Highway 567 near Busy Corner, Miss. plotted on figure 2 illustrate a typical water-surface profile along the embankment. The contracted water-surface elevation at section 3 is defined as the average of the water-surface elevations at the point where each abutment joins the downstream side of the embankment. This elevation is a close approximation of the water-surface elevation at the vena contracta. The difference between the contracted water-surface elevation and the computed-natural water-surface elevation at section 3 is  $h_3^*$ . This value is positive where the contracted water-surface elevation is greater than the computed natural water-surface elevation and negative where the contracted is less than the natural. Tables 3 and 4 contain the measured values of  $h_3^*$  for each site.

Table 3.--Summary of data for computing backwater and discharge by the Survey method

Flood no.	Type opening *	E	m	b ft	b <sub>t</sub> ft	Δh ft	L <sub>w</sub> ft	Dike Type	L <sub>d</sub> ft	b <sub>d</sub> ft	x ft	L ft	A <sub>j</sub> ft <sup>2</sup>	e	Φ	C	C <sub>I</sub>	α <sub>1</sub>	A <sub>1</sub> ft <sup>2</sup>	K <sub>1</sub> ft <sup>3</sup> /s
1	3	1.5	0.54	222	225	1.00	250	---	---	---	10	48	82	0.03	0	0.73	0.65	1.09	3,300	78,600
2	3	L4.0,R1.5	0.58	242	246	0.55	260	---	---	---	L24,R7	L55,R38	82	0.16	0	0.81	0.65	1.05	3,160	88,700
3	3	L4.0,R1.5	0.60	247	255	0.65	260	---	---	---	L14,R6	L45,R37	119	0.12	0	0.81	0.64	1.05	4,790	147,360
4	3	2.0	0.63	464	469	1.49	370	Elliptical	210	870	7	41	108	0.04	0	0.86	0.78	1.09	9,680	302,980
5	4	2.0	0.53	149	149	0.76	170	---	---	---	---	37	44	0.98	0	0.71	0.67	1.15	2,290	57,000
6	3	1.5	0.57	246	251	0.89	240	---	---	---	10	34	39	0.07	0	0.73	0.65	1.07	3,520	93,200
7	3	1.5	0.63	250	260	1.11	240	---	---	---	7	31	66	0.16	0	0.73	0.65	1.09	6,990	276,400
8	4	2.0	0.71	200	200	1.00	270	---	---	---	---	39	28	0.55	0	0.72	0.66	1.04	3,320	93,500
9	4	2.0	0.74	200	200	1.67	270	---	---	---	---	33	44	0.74	0	0.73	0.65	1.03	6,260	213,800
10	4	2.0	0.81	158	158	2.45	160	---	---	---	---	28	34	0.42	14	0.76	0.68	1.29	9,290	1,116,400
11	3	4.0	0.78	178	202	2.35	254	---	---	---	36	64	54	0.26	0	0.83	0.68	1.57	17,350	1,717,200
12	3	1.5	0.80	486	490	1.55	526	Elliptical	60	493	5	32	209	0.37	7	0.75	0.66	1.11	16,980	778,760
13	3	1.5	0.80	493	497	1.80	526	Elliptical	60	496	5	30	239	0.41	7	0.75	0.66	1.12	19,570	982,800
14	3	2.0	0.79	240	263	0.96	256	Straight	150	250	4	34	74	0.49	0	0.81	0.74	1.08	9,130	179,400
15	3	2.0	0.47	546	551	1.46	1,089	Elliptical	150	633	18	46	177	0	7	0.87	0.79	2.22	11,000	509,400
16	3	2.0	0.57	546	550	1.00	689	Elliptical	150	633	21	49	156	0.54	7	0.89	0.78	2.90	14,270	483,700
17	3	2.0	0.68	397	415	2.66	1,297	---	---	---	6	34	195	0.42	0	0.72	0.66	2.91	32,170	1,701,200
18	3	2.0	0.71	400	417	2.97	1,297	---	---	---	6	34	200	0.47	0	0.72	0.66	2.57	35,890	2,001,000
19	3	2.0	0.70	399	417	2.74	1,297	---	---	---	6	34	210	0.47	0	0.71	0.67	2.64	34,820	1,917,900
20	3	2.0	0.52	336	362	1.70	348	Elliptical	150	392	12	41	90	0.66	0	0.95	0.87	2.81	20,670	974,000
21	3	2.0	0.55	336	362	2.10	348	Elliptical	150	392	12	41	93	0.55	0	0.93	0.86	2.66	22,890	1,117,100
22	4	2.0	0.57	497	497	1.48	835	---	---	---	55	79	0.31	26	0.69	0.64	1.13	5,930	151,300	
23	4	2.0	0.60	496	496	1.70	835	---	---	---	55	86	0.28	26	0.69	0.64	1.16	7,480	210,500	
24	4	3.3	0.89	112	118	1.13	118	---	---	---	26	55	0.80	0	0.70	0.66	1.02	9,300	233,000	
25	3	2.5	0.76	108	114	1.19	103	---	---	---	23	42	22	0.54	0	0.79	0.67	1.06	2,600	51,600
26	3	2.5	0.71	150	157	0.60	106	---	---	---	32	74	121	0.40	0	0.81	0.65	1.08	6,170	229,750
27	3	2.5	0.65	205	208	0.98	265	---	---	---	19	47	162	0.50	0	0.75	0.65	1.93	4,260	227,800
28	3	2.5	0.67	210	216	1.60	270	---	---	---	15	42	196	0.56	0	0.74	0.67	1.93	5,710	395,700
29	3	2.0	0.80	266	280	2.51	260	Elliptical	110	350	3	40	66	0.34	0	0.86	0.77	1.14	17,220	660,400
30	3	2.0	0.81	266	280	2.70	260	Elliptical	110	350	3	38	74	0.33	0	0.86	0.77	1.13	19,970	824,400
31	3	2.5	0.69	518	524	1.06	520	---	---	---	16	40	187	0.72	0	0.75	0.64	1.08	11,810	327,300

\*Type 3 - Constriction with sloping embankments and sloping spillthrough abutments

\*Type 4 - Constriction with sloping embankments and vertical abutments and wing walls

L - Left embankment

R - Right embankment

Table 3.--Continued

Flood no.	$K_{1n}$ ft <sup>3</sup> /s	$A_{3n}$ ft <sup>3</sup> /s	$A_d$ ft <sup>2</sup>	$K_d$ ft <sup>3</sup> /s	$A_3$ ft <sup>2</sup>	$K_3$ ft <sup>3</sup> /s	$K_q$ ft <sup>3</sup> /s	Q ft <sup>3</sup> /s measured	Q ft <sup>3</sup> /s computed	Percent difference ft <sup>3</sup> /s	$h_1^*$ ft measured	$h_1^*$ ft computed	$h_3^*$ ft measured	$h_3^*$ ft computed
1	57,130	922	---	---	1,000	27,400	36,200	1,780	2,200	24	0.64	0.40	0.19	+0.02
2	72,200	1,100	---	---	1,220	88,900	37,500	2,250	2,360	5	0.46	0.30	0.23	+0.08
3	119,200	1,540	---	---	1,620	147,400	59,000	4,150	4,030	-3	0.68	0.42	0.35	+0.08
4	232,660	2,500	4,070	137,500	2,360	182,000	111,500	5,600	7,850	40	0.69	0.51	-0.22	+0.13
5	46,000	680	---	---	670	50,500	26,800	1,550	2,000	29	0.40	0.28	-0.11	+0.07
6	75,700	1,000	---	---	970	59,300	39,700	2,000	2,920	46	0.47	0.26	-0.12	+0.04
7	242,000	1,790	---	---	1,740	151,000	103,200	6,600	7,630	16	0.53	0.55	-0.07	-0.06
8	61,800	620	---	---	630	33,900	27,400	1,900	2,270	19	0.69	0.51	0.21	+0.12
9	133,200	1,000	---	---	1,040	62,500	55,000	4,600	5,580	21	1.36	0.88	0.28	+0.09
10	722,000	1,430	---	---	1,320	155,300	212,500	11,900	12,100	-2	1.61	1.95	-0.71	-0.36
11	839,000	1,780	---	---	2,010	263,100	376,600	16,100	18,500	15	3.08	1.81	1.16	-0.39
12	550,000	3,780	4,270	301,900	3,950	617,000	153,500	12,500	15,400	23	1.27	0.84	0.66	+0.13
13	728,900	4,170	4,470	322,500	4,320	709,100	192,100	17,900	20,000	12	1.16	1.20	0.30	+0.10
14	110,400	1,150	1,160	159,800	1,310	194,200	37,200	3,800	4,080	7	1.10	0.70	0.64	0.36
15	492,300	4,460	4,440	269,900	4,480	569,200	271,300	10,200	12,250	20	1.10	0.56	0.04	+0.10
16	384,700	4,080	3,940	228,600	4,100	515,500	208,900	8,100	10,400	28	0.50	0.37	-0.10	+0.16
17	1,105,000	4,880	---	---	4,750	710,200	543,300	25,000	35,600	42	1.60	0.89	-0.21	+0.35
18	1,136,000	5,000	---	---	4,970	750,430	586,200	31,500	40,500	29	2.18	1.25	-0.10	+0.60
19	1,329,000	5,170	---	---	4,980	755,600	572,900	31,000	38,200	23	1.40	1.26	-0.48	+0.31
20	730,394	4,320	5,280	742,900	4,450	914,800	466,200	25,600	30,700	20	1.35	0.72	0.35	+0.19
21	840,461	4,560	5,440	777,600	4,560	948,800	503,500	29,500	35,600	21	1.42	0.90	-0.02	+0.14
22	90,000	1,840	---	---	2,050	163,800	65,600	3,500	4,500	29	0.73	0.58	0.42	+1.04
23	126,000	2,040	---	---	2,240	184,100	83,400	4,900	6,240	27	0.88	0.69	0.40	+1.02
24	162,000	890	---	---	835	86,500	25,350	4,200	4,050	-4	1.22	1.03	0.20	+0.01
25	32,600	397	---	---	400	27,000	12,300	1,500	1,790	19	0.85	0.63	0.00	+0.11
26	161,000	1,960	---	---	2,040	269,250	66,300	4,740	6,730	42	1.10	0.22	0.55	+0.06
27	176,000	1,370	---	---	1,400	144,900	79,000	5,500	6,000	9	0.72	0.61	0.14	+0.02
28	313,300	1,670	---	---	1,610	180,900	129,460	9,500	10,100	6	0.86	1.04	-0.30	-0.13
29	390,000	3,000	2,960	342,600	2,880	520,400	135,000	14,200	20,200	42	1.89	0.95	0.19	+0.32
30	485,000	3,070	3,170	376,900	3,120	581,700	157,600	17,000	23,900	41	2.32	1.12	0.18	+0.26
31	257,489	2,980	---	---	2,980	237,000	100,000	6,400	7,360	+15	0.73	0.56	0.09	+0.11

Table 4.--Summary of data for computing backwater by the FHWA method

Flood no.	Abutment type	Pier type	Q ft <sup>3</sup> /s	M	S <sub>o</sub>	A <sub>1</sub> ft <sup>2</sup>	A <sub>1n</sub> ft <sup>2</sup>	A <sub>2n</sub> ft <sup>2</sup>	A <sub>4</sub> ft <sup>2</sup>	A <sub>p</sub> ft <sup>2</sup>	α <sub>1</sub>	e <sub>c</sub>	Φ	α <sub>2</sub>	K*	L* ft	L ft	b ft	h <sub>1</sub> * ft measured	h <sub>1</sub> * ft computed	h <sub>3</sub> * ft measured	h <sub>3</sub> * ft computed
1	S	B	1,780	0.46	0.0013	3,300	2,650	922	1,640	80	1.09	0.97	0	1.05	1.59	170	48	222	0.66	0.11	0.19	-0.05
2	S	A	2,250	0.42	0.0011	3,160	2,770	1,100	2,760	80	1.05	0.84	0	1.05	1.59	90	47	242	0.54	0.11	0.23	-0.04
3	S	A	4,150	0.40	0.0011	4,790	4,180	1,540	4,960	112	1.05	0.88	0	1.05	1.69	160	41	247	0.52	0.20	0.35	-0.06
4	S	C	5,600	0.37	0.0010	9,680	7,020	2,500	5,320	111	1.09	0.06	0	1.05	1.75	160	41	464	1.17	0.16	-0.22	-0.04
5	W	B	1,550	0.47	0.0016	2,290	1,980	680	1,700	44	1.15	0.02	0	1.05	1.37	40	37	149	0.48	0.12	-0.11	-0.05
6	S	C	2,000	0.43	0.0014	3,520	3,080	1,000	3,020	45	1.07	0.93	0	1.05	1.58	165	34	246	0.39	0.10	-0.12	-0.04
7	S	C	6,600	0.37	0.0015	6,990	6,400	1,790	5,920	74	1.09	0.84	0	1.05	1.75	220	31	250	0.67	0.39	-0.07	-0.11
8	W	A	1,900	0.29	0.0016	3,320	2,540	620	1,600	25	1.04	0.45	0	1.00	2.10	80	39	200	1.01	0.32	0.21	-0.06
9	W	A	4,600	0.26	0.0016	3,260	4,600	1,000	3,140	42	1.03	0.26	0	1.00	2.24	145	33	200	1.65	0.74	0.28	-0.12
10	W		12,100	0.19	0.0010	9,290	7,100	1,430	5,970	34	1.29	0.58	14	1.05	2.49	165	28	158	1.65	2.96	-0.71	-0.32
11	S		16,100	0.22	0.0010	17,350	10,700	1,780	9,800	54	1.57	0.74	0	1.10	2.42	225	64	178	3.16	3.43	1.16	-0.45
12	S	D	12,500	0.20	0.0009	16,980	---	3,780	9,400	209	1.11	0.63	7	1.00	2.59	260	32	486	2.68	0.46	0.66	-0.05
13	S	D	17,900	0.20	0.0009	19,570	---	4,170	11,300	239	1.12	0.59	7	1.00	2.59	335	30	493	2.58	0.77	0.30	-0.09
14	S	B	3,800	0.21	0.0005	9,130	6,690	1,150	9,200	74	1.08	0.51	0	1.00	2.56	110	34	240	0.89	0.43	0.64	-0.05
15	S	B-15, D-7	10,200	0.53	0.0005	11,000	---	4,460	12,600	177	2.22	1.00	7	1.60	1.26	395	46	546	1.16	0.15	0.04	-0.06
16	S	B-15, D-7	8,100	0.43	0.0005	14,270	---	4,080	10,700	156	2.90	0.46	7	1.80	1.47	165	49	546	0.75	0.18	-0.10	-0.07
17	S	A	25,000	0.32	0.0011	32,170	24,000	4,880	21,000	190	2.91	0.58	0	1.60	1.95	310	34	397	2.15	1.33	-0.21	-0.29
18	S	A	31,500	0.29	0.0011	35,890	24,670	5,000	22,000	200	2.57	0.53	0	1.45	2.10	350	34	400	2.83	2.15	1.95	-0.37
19	S	A	31,000	0.30	0.0011	34,820	27,400	5,170	24,000	210	2.64	0.53	0	1.50	2.05	350	34	399	2.02	1.77	-0.48	-0.35
20	S	D	25,600	0.48	0.0010	20,670	---	4,320	12,700	90	2.81	0.34	0	1.90	1.23	300	41	336	1.59	1.48	0.35	-0.61
21	S	D	29,500	0.45	0.0010	22,890	---	4,560	14,600	93	2.66	0.45	0	1.75	1.35	300	41	336	1.25	1.71	-0.02	-0.64
22	W	B	3,500	0.43	0.0010	5,930	4,160	1,840	5,200	79	1.13	0.69	26	1.05	1.37	140	55	497	2.29	0.08	0.42	-0.03
23	W	B	4,900	0.40	0.0010	7,480	5,231	2,040	5,500	86	1.16	0.72	26	1.05	1.48	245	55	496	2.45	0.15	0.40	-0.05
24	W	A	4,200	0.11	0.0009	9,300	7,450	890	6,740	55	1.02	0.80	0	1.00	3.06	100	26	112	1.53	1.06	0.20	-0.04
25	S	A	1,500	0.24	0.0016	2,600	1,920	397	1,320	22	1.06	0.46	0	1.00	2.38	65	42	108	0.98	0.54	0.00	-0.08
26	S	C	4,740	0.29	0.0011	6,170	4,570	1,960	5,750	121	1.08	0.60	0	1.00	2.16	55	74	150	1.30	0.20	0.55	-0.04
27	S	C	5,500	0.35	0.0014	4,260	3,600	1,370	2,300	167	1.93	0.50	0	1.30	1.95	150	47	205	0.79	0.79	0.14	-0.19
28	S	C	9,500	0.33	0.0014	5,710	4,920	1,670	3,400	216	1.93	0.44	0	1.30	2.05	180	42	210	0.97	1.54	-0.30	-0.33
29	S	D	14,200	0.20	0.0010	17,220	---	3,000	7,460	66	1.14	0.62	0	1.00	2.56	165	40	266	2.17	0.94	0.19	-0.11
30	S	D	17,000	0.19	0.0010	19,970	---	3,070	9,480	74	1.13	0.51	0	1.00	2.61	195	38	266	2.60	1.29	0.18	-0.13
31	S	C	6,400	0.31	0.0008	11,810	10,060	2,980	8,030	187	1.08	0.28	0	1.00	2.07	165	40	518	1.12	0.15	0.09	-0.03

A - Round piles, three per bent  
 B - Round piles, four per bent  
 C - Square piles, three per bent  
 D - Square piles, four per bent  
 S - Spillthrough abutments  
 W - 45° wing wall abutments

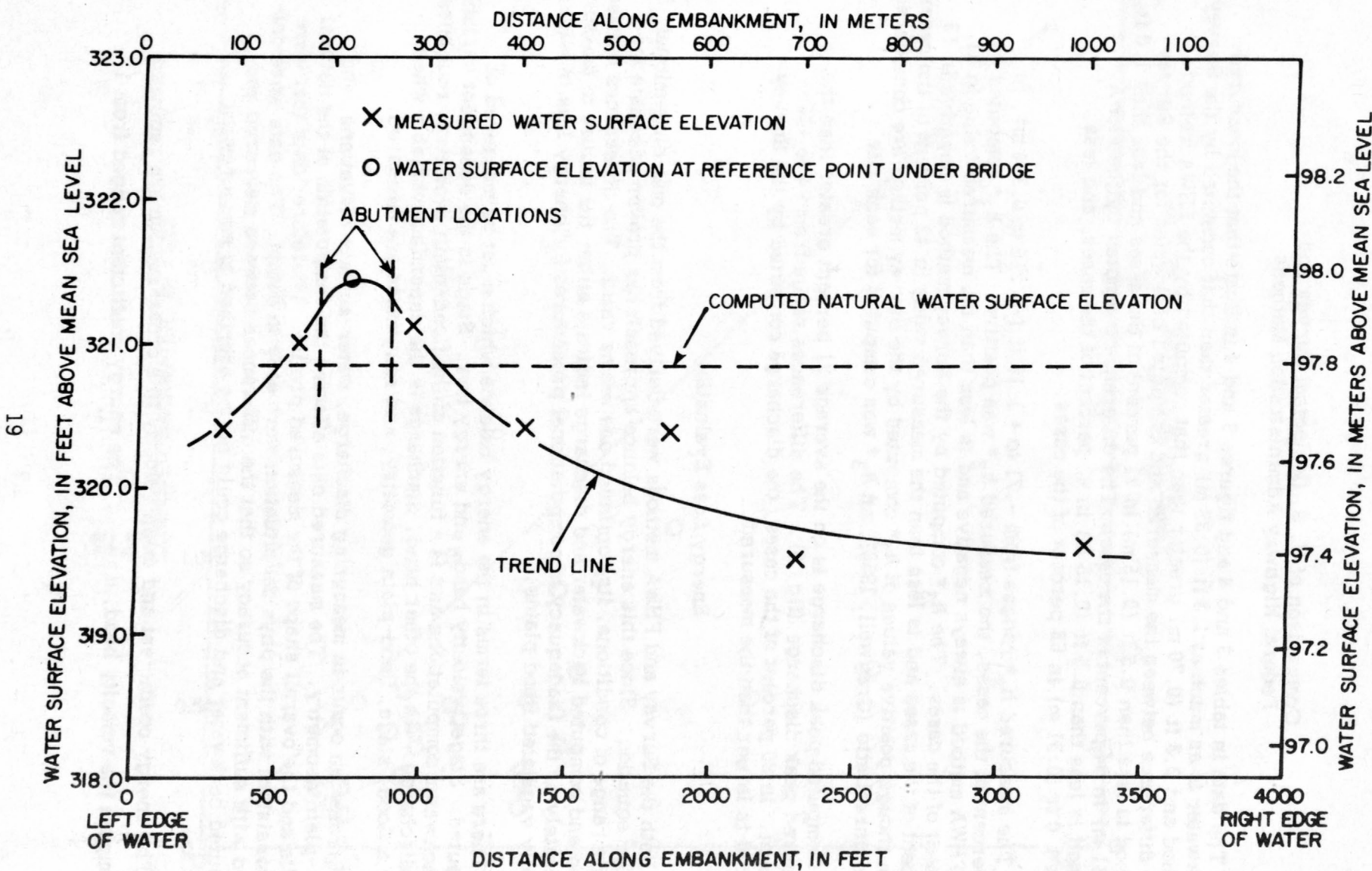


Figure 2.--Water-surface elevation on the downstream side of the right embankment, West Fork Amite River, near Busy Corner, Mississippi, December 6, 1972.

## Comparison of U. S. Geological Survey and Federal Highway Administration Methods

The data in tables 3 and 4 and figures 3 and 4 indicate that the measured backwater is as much as 1.3 ft (0.39 m) greater than that computed by the Survey method and 2.3 ft (0.70 m) greater than that computed by the FHWA method. The difference between the measured and computed backwater for the Survey method is less than 0.5 ft (0.15 m) in 71 percent of the cases and less than 1.0 ft (0.31 m) in 94 percent of the cases. The difference computed by the FHWA method is less than 0.5 ft (0.15 m) in 42 percent of the cases, and less than 1.0 ft (0.31 m) in 68 percent of the cases.

The measured  $h_3^*$  ranges from - .71 to + 1.16 ft (-0.216 to 0.354 m). In 65 percent of the cases, the measured  $h_3^*$  was positive. The  $h_3^*$  computed by the FHWA method is always negative and is less than the measured value in 81 percent of the cases. The  $h_3^*$  computed by the Survey method is negative in 13 percent of the cases and is less than the measured value in 42 percent of the cases. Even though positive values of  $h_3^*$  computed by the Survey method are considered to be unrealistic (Cragwall, 1958), an  $h_3^*$  was computed for each site.

Computed peak discharge is on the average 21 percent greater than the measured peak discharge (fig. 5). The differences range from -4 to +46 percent. In 90 percent of the cases, the discharge computed by the Survey method is larger than the measured.

### Energy Loss Evaluation

Both the Survey and FHWA methods were derived from the one-dimensional energy equation. Since this energy balance approach has proven adequate for a wide range of conditions, its continued use seems valid. The differences between measured and computed backwater and discharge indicate either the failure to measure accurately or the inadequacy of computational procedures for energy loss in wide, heavily vegetated flood plains.

There are three terms in the energy balance which must be measured or computed: Stage, velocity head, and energy loss. Stage is the dependent variable in backwater computations and is a function of the flood-plain geometry, roughness, and discharge. On the other hand, discharge is the dependent variable when after a flood, stage, flood-plain geometry, and roughness are measured.

Errors can occur in measuring discharge, water-surface elevations, and flood-plain geometry. The measured data affected the computation of the natural profile and the overall shape of the measured profile. Therefore, data that were not consistent with the physical situation were easy to detect. The data were collected with sufficient accuracy so that the differences between measured and computed backwater and discharge could not be ascribed to measurement errors.

The energy coefficient and mean velocity in a cross-section are required to compute the velocity head,  $\alpha \frac{V^2}{2g}$ . The energy coefficient ranged from 1

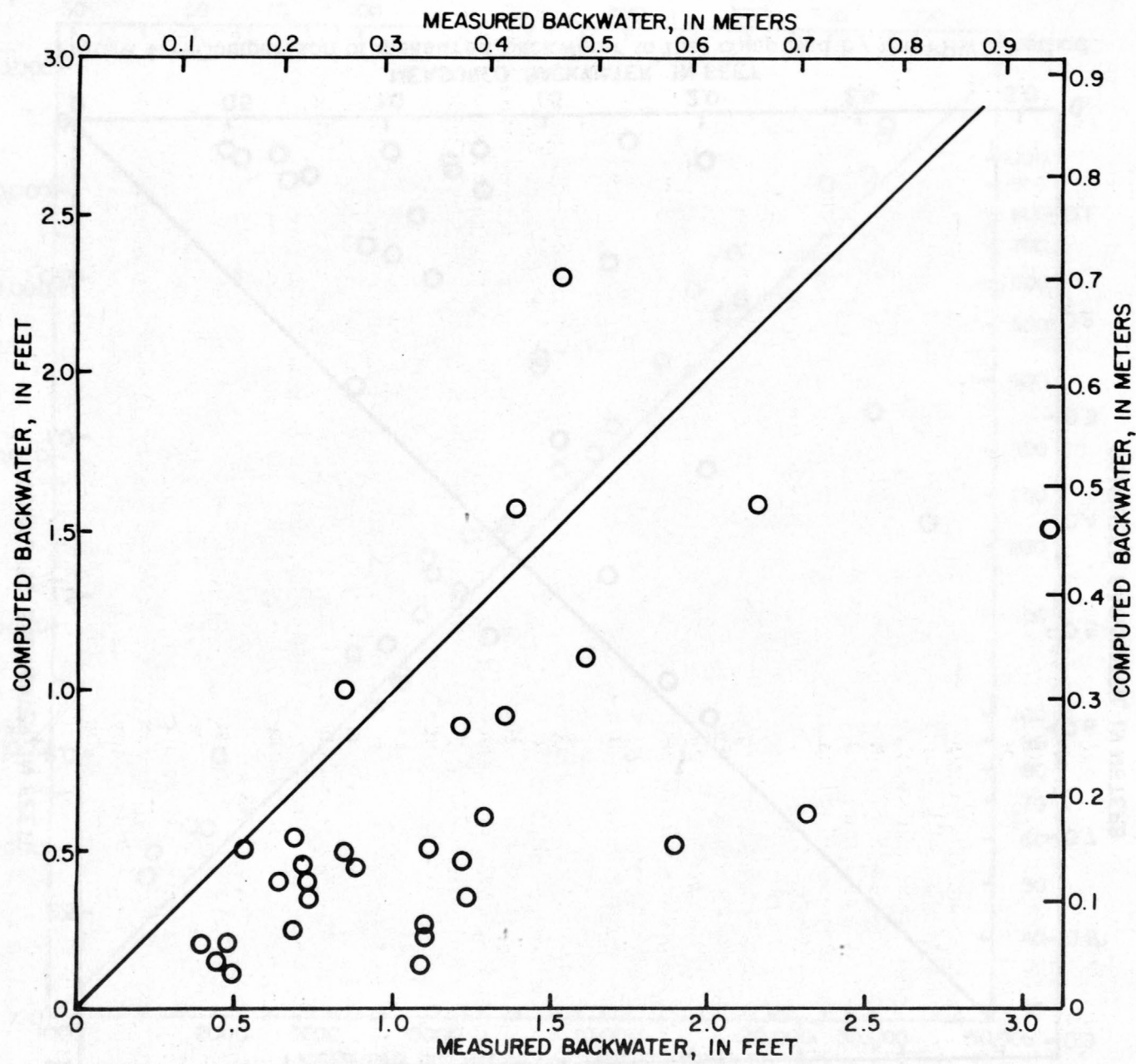


Figure 3.--Comparison of measured backwater to that computed by the Survey method.

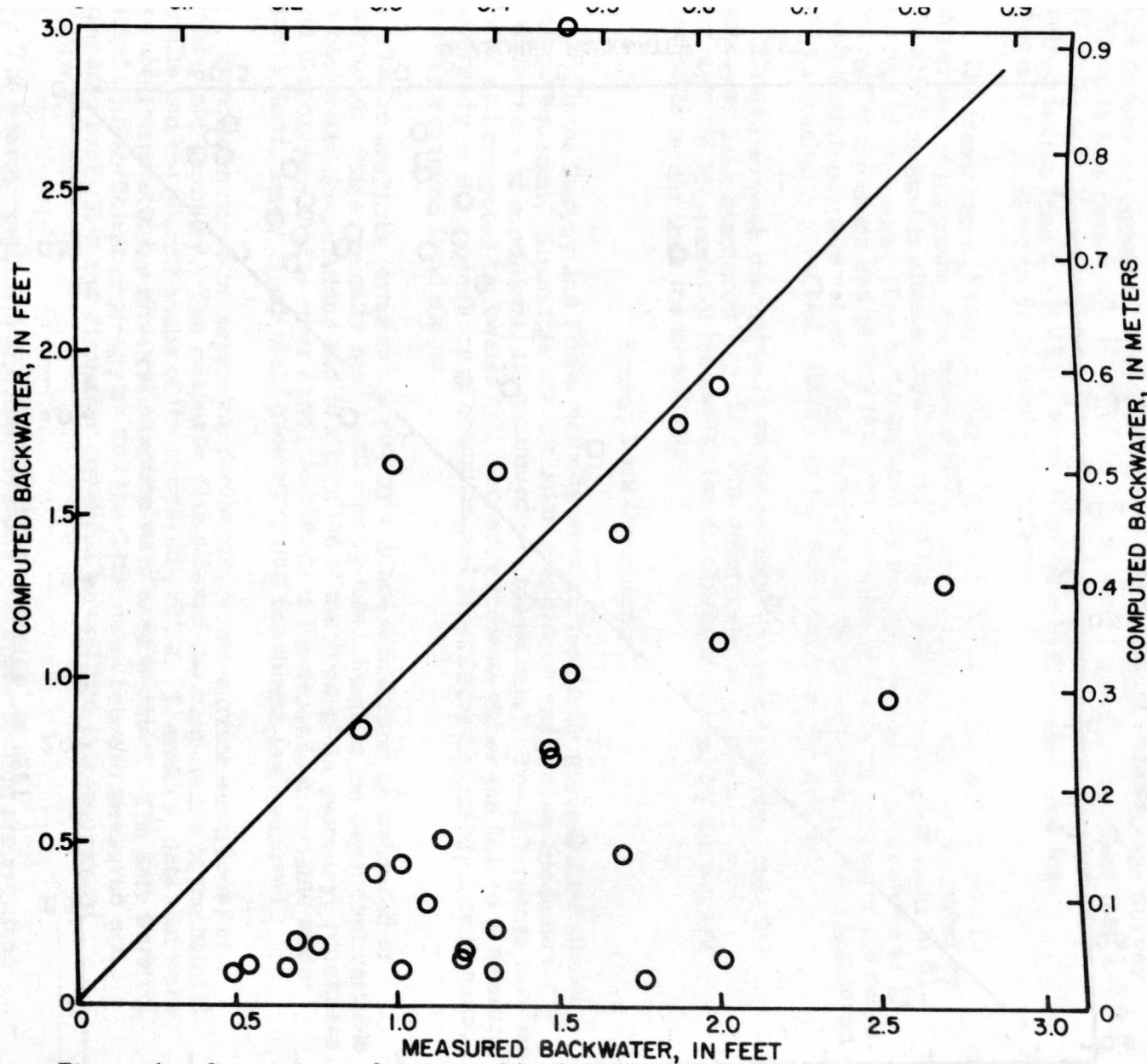


Figure 4.--Comparison of measured backwater to that computed by the FHWA method.

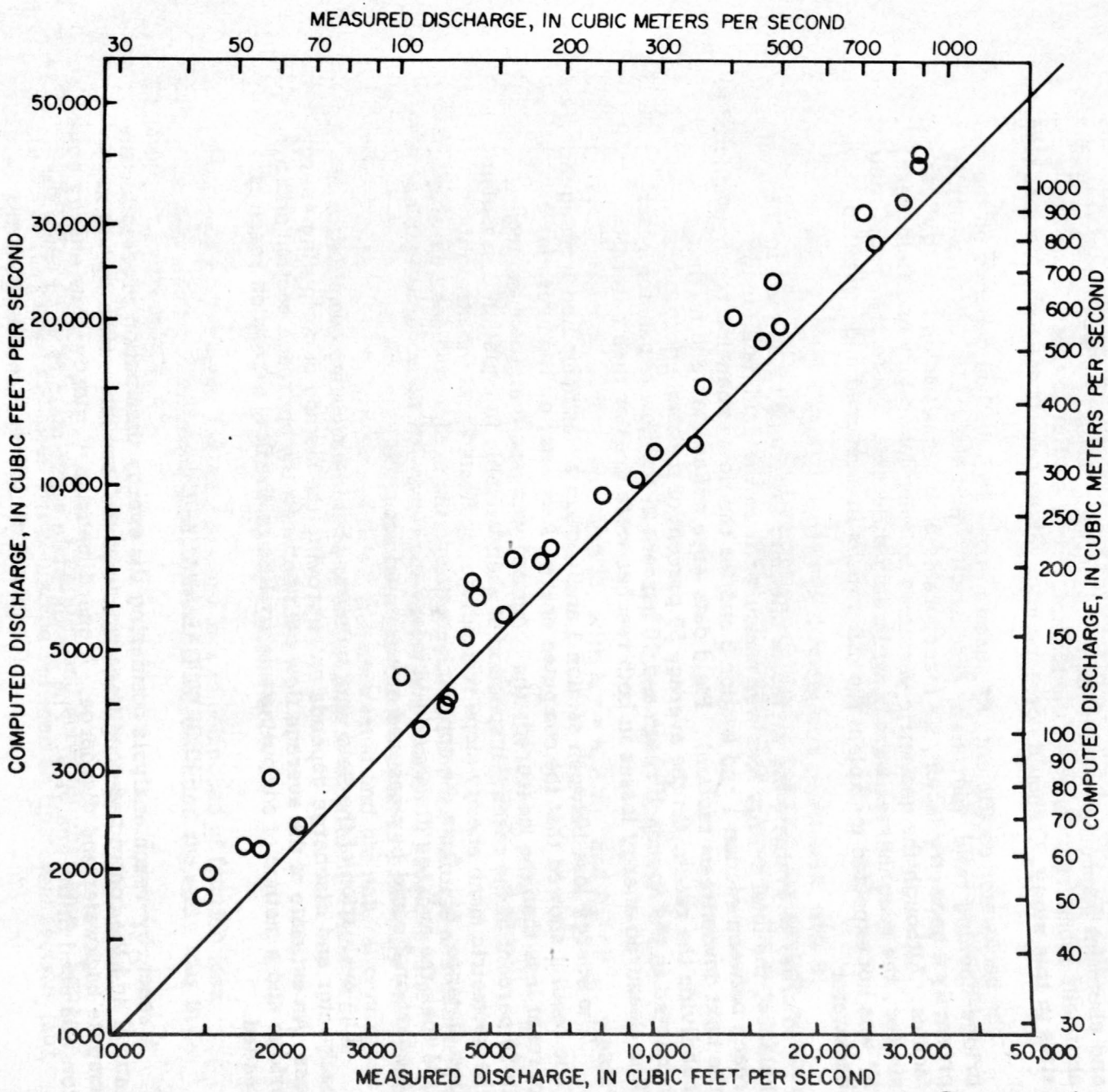


Figure 5.--Comparison of measured discharge to that computed by the Survey method.

to 8 at the study sites. However, because the mean velocities were usually less than 1 ft/s, the velocity head was often less than 0.1 ft (30 mm) at the valley cross sections. Therefore, errors in computing the velocity head were not a significant component of the difference between computed and measured backwater and discharge.

The discharge coefficient  $C$ , in equation 1 is primarily a measure of the vena contracta width in relation to the bridge opening width, even though  $C$  includes a coefficient for minor eddy losses. As such,  $C$  is a function of bridge and abutment geometry, (Kindsvater and Carter, 1955). Because the bridge and abutment geometries tested in the laboratory are similar to those found at the sites in this study,  $C$  should correspond to values recommended by Matthai (1967).

The backwater coefficient,  $K^*$ , used in the FHWA method depends on the bridge-opening ratio, pier area, eccentricity, and skew. Unlike  $C$ , which is primarily a geometry factor,  $K^*$  incorporates both geometric and energy loss factors. Although the geometric variables between laboratory and field were similar, the roughnesses were considerably different. Therefore, redefining  $K^*$  was not expected to explain the differences in measured and computed backwater.

In order to evaluate the variables affecting the energy loss term in the balance, the total energy loss was measured from the field data for the reach between section 1 and section 3 and for the flow expansion reach (section 3 to the next downstream section). Field data were not available to further subdivide the reach. On the average 50 percent of the total energy loss occurred in the approach reach and 50 percent in the flow expansion reach. The measured energy losses in both reaches were greater than natural.

The energy loss between section 1 and section 3 was computed from equation 2. The results showed that the computed energy loss was, on the average, 37 percent less than the measured; the computed was less than the measured in 90 percent of the cases. Inspection of each variable in equation 2, assuming the geometric mean energy slope is accurate, indicated that the straight-line distance,  $L_w$ , from the approach section to the bridge was considerably less than the average distance traveled by the flow. All the other variables in equation 2 could be measured or computed accurately.

The evaluation of the field data indicates that the accurate computation of backwater and discharge depends on improving the method of computing energy loss. An estimate of the average flow path between the approach section and the bridge and a method of computing energy loss in the flow expansion reach is needed.

#### THEORETICAL ANALYSIS

A reach-by-reach analysis comparing the energy dissipation process for the natural and the contracted conditions was used to formulate a new method to compute backwater and discharge. A one-dimensional, steady-state energy equation was used in the analysis. The steady-state assumption is valid when the

peak flow is of long duration and the total runoff is much greater than the valley storage. Figure 6 illustrates a study reach with cross-section locations. Section 1 is the approach section and is ideally located at the point of maximum backwater and in a region of one-dimensional flow. Section d is the dike section if spur dikes are present. It is located at the toe of the spur dikes; properties subscripted with a "d" refer to the dike section. Section 2 is located at the upstream face of the bridge, and section 3 is located at the most contracted section, as described by Matthai (1967). Section 4 is located at the downstream section where the contracted flow returns to natural elevation. A geometric constriction ratio,  $m^1$ , a function of the bridge width,  $b$ , and the valley width,  $B$ , is defined as

$$m^1 = 1 - b/B \quad (11)$$

The energy equation between sections 1 and 4 for natural (unconstricted) conditions is

$$h_{1n} + \alpha_{1n} \frac{V_{1n}^2}{2g} = h_{4n} + \alpha_{4n} \frac{V_{4n}^2}{2g} + h_L(1 - 4)n \quad (12)$$

where  $h$  is stage,  $V$  is velocity,  $\alpha$  is energy distribution coefficient, and  $h_L$  is head loss from all sources. The numerical subscript refers to the section number, and  $n$  refers to the natural condition. With the constriction in place, the energy equation is

$$h_1 + \alpha_1 \frac{V_1^2}{2g} = h_4 + \alpha_4 \frac{V_4^2}{2g} + h_L(1 - d) + h_L(d - 2) + h_L(2 - 3) + h_L(3 - 4) \quad (13)$$

Subtraction of equation 12 from equation 13, with  $h_1^* = h_1 - h_{1n}$  and  $h_4 = h_{4n}$ , yields

$$h_1^* + \left[ \alpha_1 \frac{V_1^2}{2g} - \alpha_{1n} \frac{V_{1n}^2}{2g} \right] = h_L(1 - d) + h_L(d - 2) + h_L(2 - 3) + h_L(3 - 4) - h_L(1 - 4)n \quad (14)$$

The difference between velocity heads at section 1 for the natural and constricted conditions is small for wide, heavily vegetated flood plains. Therefore, the backwater caused by the constriction at the approach section is primarily attributable to the difference in total energy losses for the contracted and the natural conditions. Improved estimates of the energy losses are required to accurately estimate backwater.

### Energy Losses in Approach Reach

In the approach reach, the total energy loss is composed of friction loss and eddy loss terms. Kindsvater and Carter (1955) included the eddy loss in the discharge coefficient,  $C$ .

In order to estimate the friction slope in gradually varied flow, assume the uniform flow equation ( $Q = K S_f^{1/2}$ ) applies and solve for the slope. Equation 15 gives the geometric mean friction slope between an upstream section (subscript  $i$ ) and a downstream section (subscript  $j$ ).

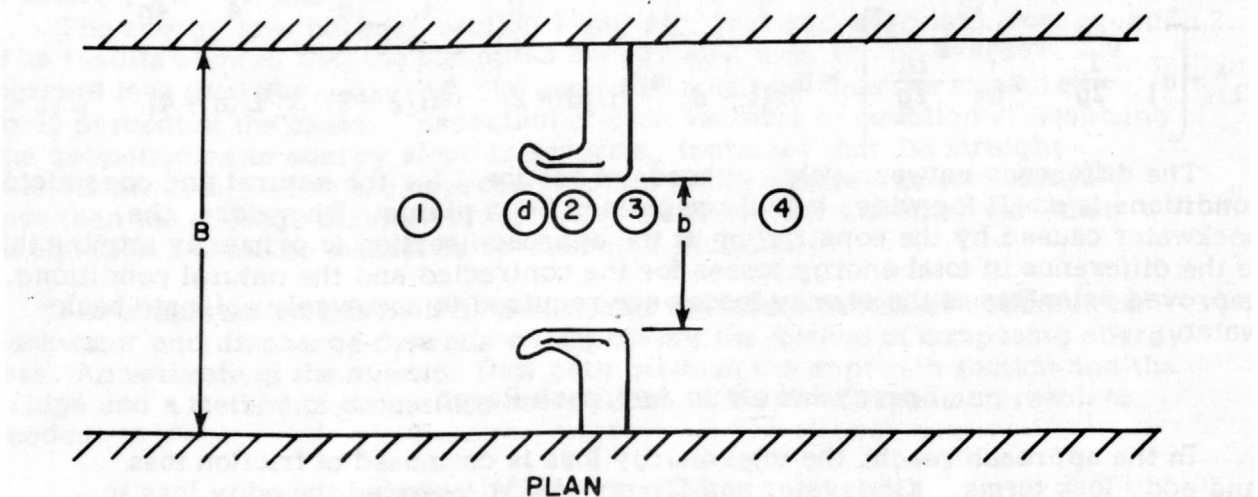
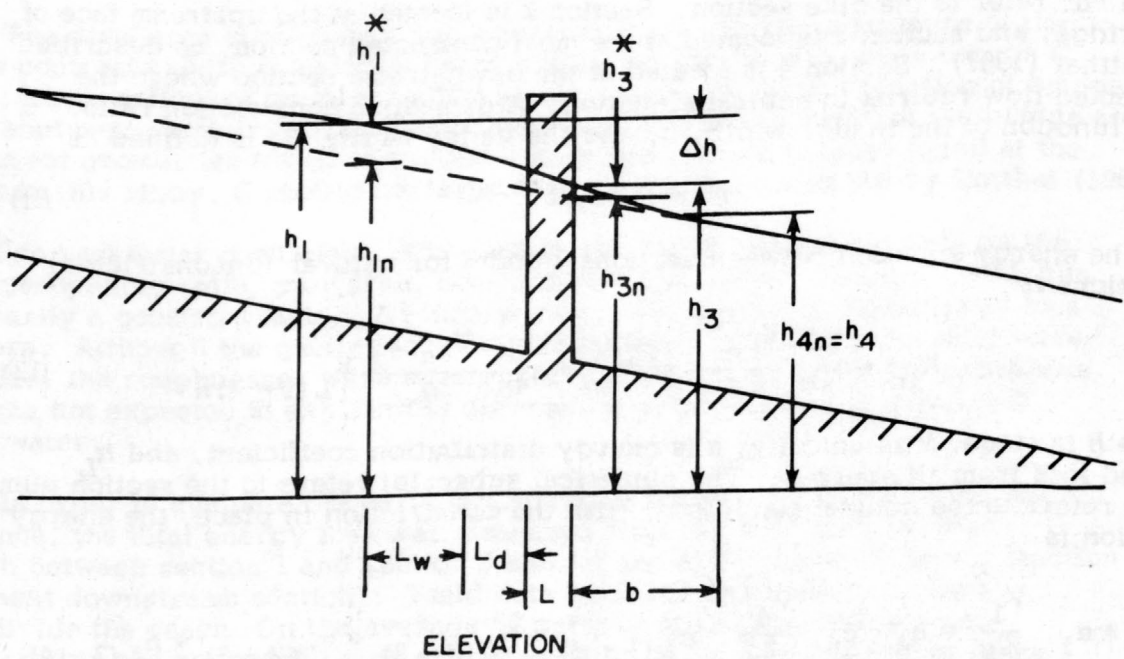


Figure 6.--Definition sketch of the variables used in computing backwater and discharge by the proposed method.

$$S_{f(i-j)} = \frac{Q^2}{K_i K_j} \quad (15)$$

where  $Q$  is discharge,  $S_f$  is friction slope, and  $K$  is conveyance. The conveyance is a measure of the water-carrying capacity of the channel section. With Manning's  $n$  as the roughness coefficient,  $R$  the hydraulic radius, and  $A$  the area,  $K = 1.486 \frac{AR^{2/3}}{n}$ . Multiplication of the friction slope,  $S_f$ , by the average length of the streamline,  $L_w$ , gives the head loss,  $h_f$ , for the reach

$$h_{f(i-j)} = L_w(i-j) S_{f(i-j)} \quad (16)$$

For unstricted flow, or for small constriction ratios, the straight-line distance is an adequate estimate of the streamline length. However, for large constriction ratios, the average streamline length is much greater than the straight-line distance between section 1 and section 2. To determine the average streamline length required in equation 16, Su (1973) studied an idealized constriction using potential flow theory.

A potential flow field past a symmetric constriction was considered. The analysis used a Schwartz-Christoffel transformation (Churchill and others, 1948) of a potential source in a half plane ( $W$  plane) to the flow field with boundaries representing those in open-channel flow ( $Z$  plane) (fig. 7). An example solution for a constriction ratio ( $m'$ ) of 0.8 is presented in figure 8.

The average streamline length as a function of the distance upstream to the approach section,  $L_w$ , could be determined for each constriction ratio by averaging the lengths of the individual streamlines. Figure 9 and table 5 present the solution and are used to determine the average length of flow,  $L_{av}$ , required to compute the friction losses in the approach reach (eq. 17).

$$h_{L(1-2)} = L_{av(1-2)} S_{f(1-2)} \quad (17)$$

The one-dimensional energy equation requires that section 1 be located in a zone of nearly one-dimensional flow. The potential flow field was studied in order to define a consistent location. The approach section is located at the intersection of the center streamline and the equipotential line drawn through the point where the edge of water and embankment intersects. The distance to the approach section can be computed from equation 18.

$$\frac{L_w}{b} = \frac{1}{\pi(1-m')} \left\{ \frac{1}{2} \ln \left[ \left( \sqrt{\frac{8}{\varepsilon^2}} + 8 - \frac{3}{\varepsilon} - \varepsilon \right) \left( -\sqrt{8 + 8\varepsilon^2} - 3\varepsilon - \frac{1}{\varepsilon} \right) \right] - \ln \left( \varepsilon - \frac{1}{\varepsilon} \right) \right\} \quad (18)$$

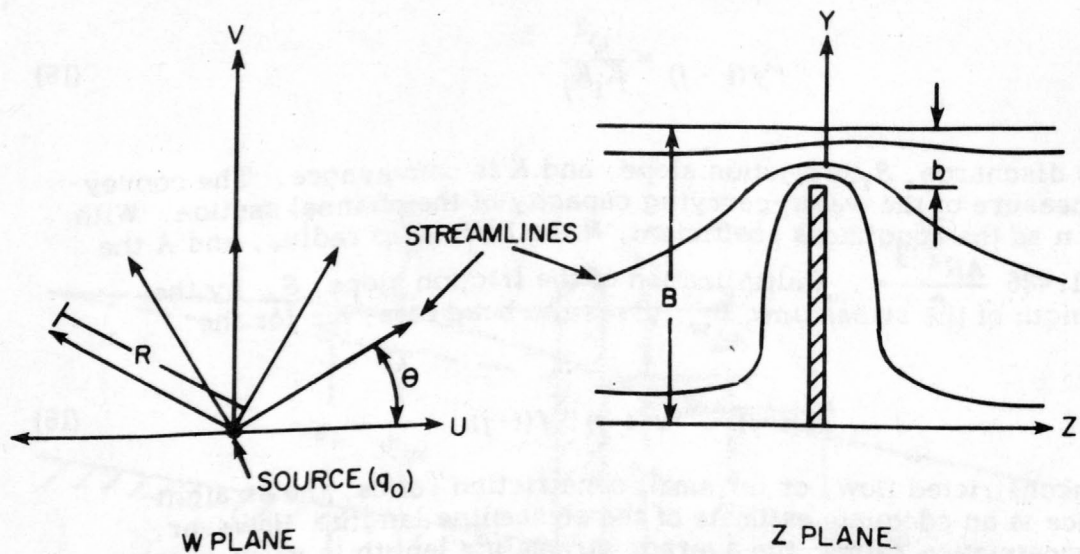


Figure 7.--W and Z planes for the Schwartz-Christoffel transformation.

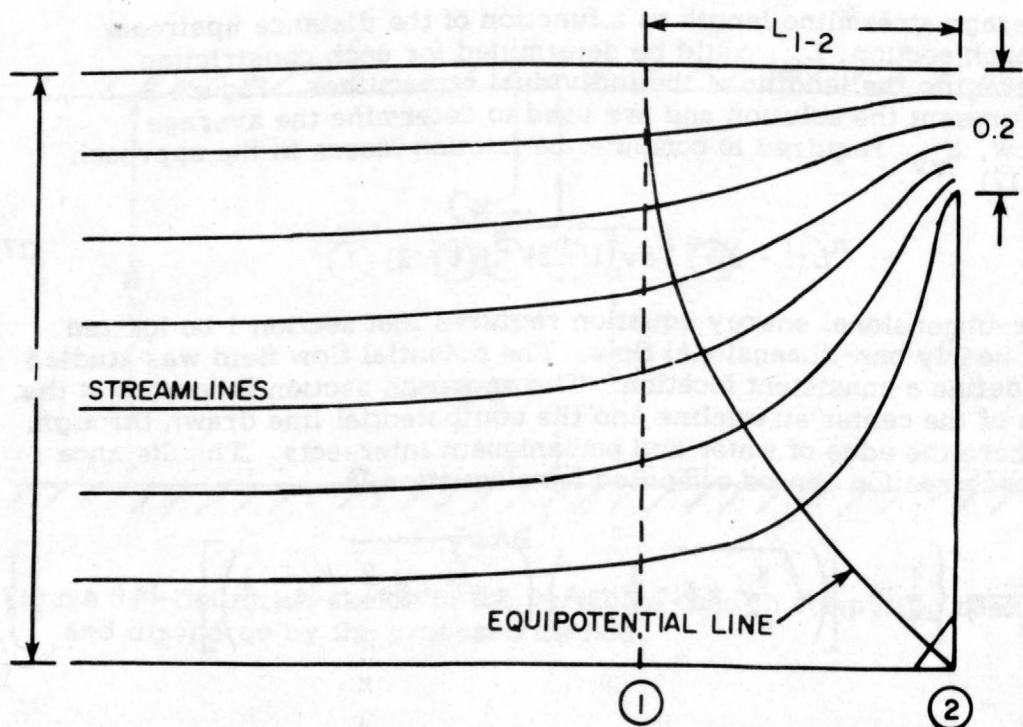
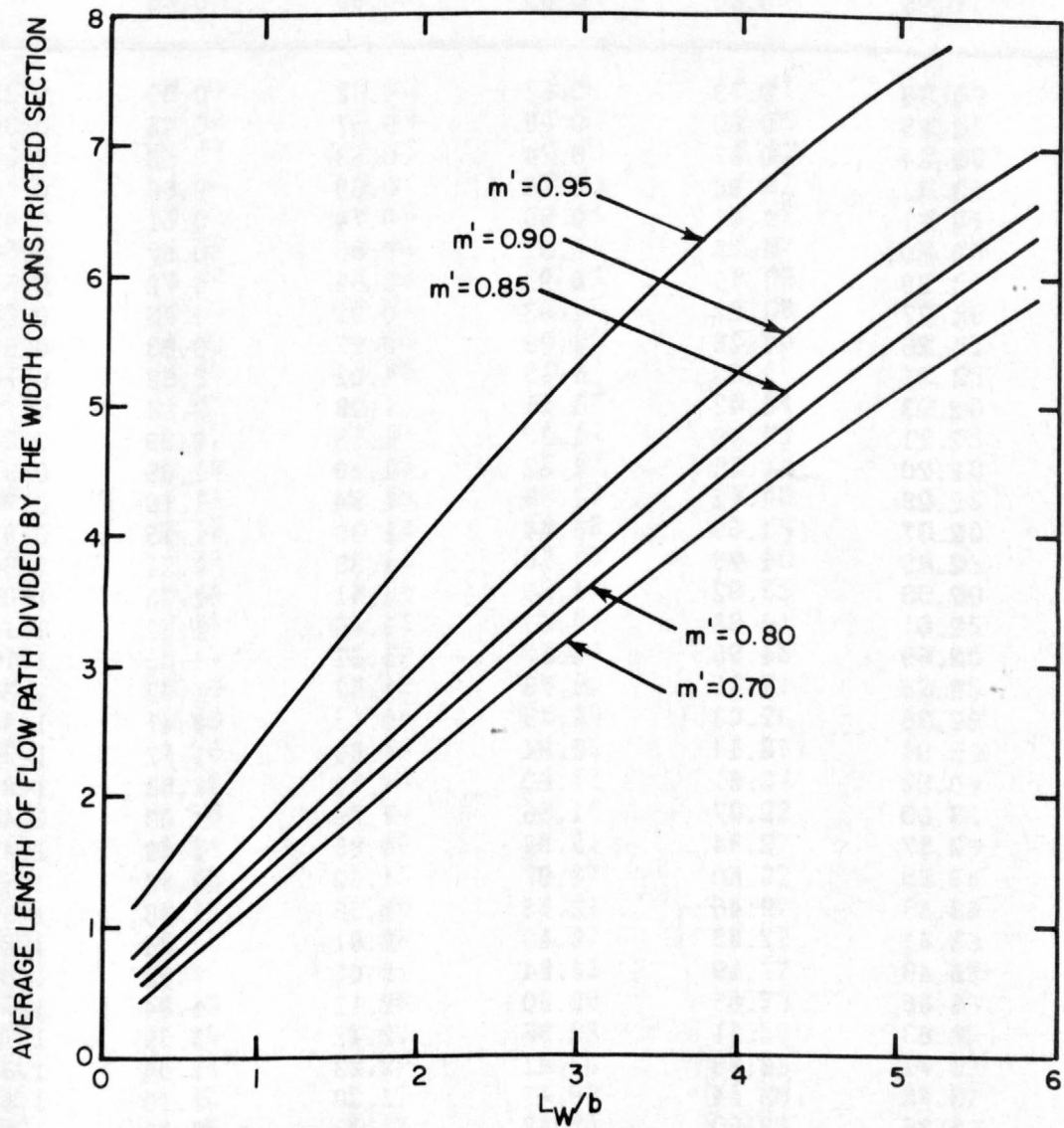


Figure 8.--Flow pattern for one-half of a symmetric constriction developed from the potential flow model ( $m = 0.80$ ).



PERPENDICULAR DISTANCE TO THE APPROACH CROSS SECTION DIVIDED BY THE WIDTH OF THE CONSTRICTED SECTION

Figure 9.--Ratio of the average flow path length in the approach reach and the width of the constricted section as a function of the geometric constriction ratio and the ratio of the distance to the approach cross section and the width of the constriction.

Table 5.--Ratio of the average flow path length in the approach reach and the width of the constricted section as a function of the geometric constriction ratio and the ratio of the distance to the approach cross section and the width of the constriction

$L_w/b$	Geometric constriction ratio, $m^1$					$L_w/b$
	0.95	0.90	0.85	0.80	0.70	
0.25	1.16	0.73	0.62	0.52	0.39	0.25
0.30	1.25	0.80	0.68	0.57	0.45	0.30
0.35	1.34	0.87	0.74	0.63	0.50	0.35
0.40	1.42	0.94	0.79	0.69	0.56	0.40
0.45	1.51	1.01	0.85	0.74	0.61	0.45
0.50	1.60	1.08	0.91	0.80	0.67	0.50
0.55	1.69	1.15	0.97	0.85	0.72	0.55
0.60	1.77	1.22	1.03	0.91	0.78	0.60
0.65	1.86	1.28	1.09	0.97	0.83	0.65
0.70	1.95	1.35	1.15	1.02	0.88	0.70
0.75	2.03	1.42	1.21	1.08	0.94	0.75
0.80	2.11	1.49	1.27	1.13	0.99	0.80
0.85	2.20	1.55	1.32	1.19	1.05	0.85
0.90	2.28	1.62	1.38	1.24	1.10	0.90
0.95	2.37	1.69	1.44	1.30	1.15	0.95
1.00	2.45	1.75	1.50	1.35	1.21	1.00
1.05	2.53	1.82	1.56	1.41	1.26	1.05
1.10	2.61	1.88	1.61	1.46	1.31	1.10
1.15	2.69	1.95	1.67	1.52	1.36	1.15
1.20	2.78	2.01	1.73	1.57	1.42	1.20
1.25	2.86	2.08	1.79	1.63	1.47	1.25
1.30	2.94	2.14	1.84	1.68	1.52	1.30
1.35	3.02	2.21	1.90	1.74	1.58	1.35
1.40	3.09	2.27	1.96	1.79	1.63	1.40
1.45	3.17	2.34	2.02	1.85	1.68	1.45
1.50	3.25	2.40	2.07	1.90	1.73	1.50
1.55	3.33	2.46	2.13	1.95	1.78	1.55
1.60	3.41	2.53	2.19	2.01	1.84	1.60
1.65	3.48	2.59	2.24	2.06	1.89	1.65
1.70	3.56	2.65	2.30	2.12	1.94	1.70
1.75	3.63	2.71	2.36	2.17	1.99	1.75
1.80	3.71	2.78	2.41	2.23	2.04	1.80
1.85	3.78	2.84	2.47	2.28	2.10	1.85
1.90	3.86	2.90	2.52	2.33	2.15	1.90
1.95	3.93	2.96	2.58	2.39	2.20	1.95
2.00	4.01	3.02	2.64	2.44	2.25	2.00
2.05	4.08	3.08	2.69	2.49	2.30	2.05
2.10	4.15	3.15	2.75	2.55	2.35	2.10
2.15	4.22	3.21	2.80	2.60	2.40	2.15
2.20	4.30	3.27	2.86	2.66	2.45	2.20

Table 5.--Continued

$L_w/b$	Geometric constriction ratio, $m'$					$L_w/b$
	0.95	0.90	0.85	0.80	0.70	
2.25	4.37	3.33	2.91	2.71	2.50	2.25
2.30	4.44	3.39	2.97	2.76	2.55	2.30
2.35	4.51	3.45	3.03	2.82	2.60	2.35
2.40	4.58	3.51	3.08	2.87	2.66	2.40
2.45	4.65	3.56	3.14	2.92	2.71	2.45
2.50	4.72	3.62	3.19	2.97	2.76	2.50
2.55	4.78	3.68	3.24	3.03	2.81	2.55
2.60	4.85	3.74	3.30	3.08	2.86	2.60
2.65	4.92	3.80	3.35	3.13	2.91	2.65
2.70	4.99	3.86	3.41	3.19	2.95	2.70
2.75	5.05	3.91	3.46	3.24	3.00	2.75
2.80	5.12	3.97	3.52	3.29	3.05	2.80
2.85	5.19	4.03	3.57	3.34	3.10	2.85
2.90	5.25	4.09	3.63	3.40	3.15	2.90
2.95	5.32	4.14	3.68	3.45	3.20	2.95
3.00	5.38	4.20	3.73	3.50	3.25	3.00
3.05	5.44	4.25	3.79	3.55	3.30	3.05
3.10	5.51	4.31	3.84	3.61	3.35	3.10
3.15	5.57	4.37	3.89	3.66	3.40	3.15
3.20	5.63	4.42	3.95	3.71	3.45	3.20
3.25	5.69	4.48	4.00	3.76	3.49	3.25
3.30	5.76	4.53	4.05	3.81	3.54	3.30
3.35	5.82	4.59	4.11	3.87	3.59	3.35
3.40	5.88	4.64	4.16	3.92	3.64	3.40
3.45	5.94	4.69	4.21	3.97	3.69	3.45
3.50	6.00	4.75	4.27	4.02	3.74	3.50
3.55	6.06	4.80	4.32	4.07	3.78	3.55
3.60	6.11	4.86	4.37	4.12	3.83	3.60
3.65	6.17	4.91	4.42	4.17	3.88	3.65
3.70	6.23	4.96	4.48	4.23	3.93	3.70
3.75	6.29	5.02	4.53	4.28	3.97	3.75
3.80	6.34	5.07	4.58	4.33	4.02	3.80
3.85	6.40	5.12	4.63	4.38	4.07	3.85
3.90	6.46	5.17	4.68	4.43	4.12	3.90
3.95	6.51	5.22	4.74	4.48	4.16	3.95
4.00	6.57	5.28	4.79	4.53	4.21	4.00
4.05	6.62	5.33	4.84	4.58	4.26	4.05
4.10	6.68	5.38	4.89	4.63	4.30	4.10
4.15	6.73	5.43	4.94	4.69	4.35	4.15
4.20	6.78	5.48	4.99	4.74	4.40	4.20
4.25	6.84	5.53	5.04	4.79	4.44	4.25

Table 5.--Continued

$L_w/b$	Geometric constriction ratio, $m^1$					$L_w/b$
	0.95	0.90	0.85	0.80	0.70	
4.30	6.89	5.58	5.09	4.84	4.49	4.30
4.35	6.94	5.63	5.15	4.89	4.53	4.35
4.40	6.99	5.68	5.20	4.94	4.58	4.40
4.45	7.04	5.73	5.25	4.99	4.63	4.45
4.50	7.09	5.78	5.30	5.04	4.67	4.50
4.55	7.14	5.83	5.35	5.09	4.72	4.55
4.60	7.19	5.87	5.40	5.14	4.76	4.60
4.65	7.24	5.92	5.45	5.19	4.81	4.65
4.70	7.29	5.97	5.50	5.24	4.86	4.70
4.75	7.34	6.02	5.55	5.29	4.90	4.75
4.80	7.38	6.07	5.60	5.34	4.95	4.80
4.85	7.43	6.11	5.65	5.39	4.99	4.85
4.90	7.48	6.16	5.70	5.44	5.04	4.90
4.95	7.52	6.21	5.75	5.49	5.08	4.95
5.00	7.57	6.26	5.80	5.54	5.13	5.00
5.05	7.62	6.30	5.85	5.59	5.17	5.05
5.10	7.66	6.35	5.90	5.64	5.21	5.10
5.15	7.70	6.39	5.95	5.68	5.26	5.15
5.20	7.75	6.44	6.00	5.73	5.30	5.20
5.25	7.79	6.48	6.04	5.78	5.35	5.25
5.30	7.83	6.53	6.09	5.83	5.39	5.30
5.35	7.88	6.58	6.14	5.88	5.44	5.35
5.40	7.92	6.62	6.19	5.93	5.48	5.40
5.45	7.96	6.66	6.24	5.98	5.52	5.45
5.50	8.00	6.71	6.29	6.03	5.57	5.50
5.55	8.04	6.75	6.34	6.08	5.61	5.55
5.60	8.08	6.80	6.38	6.13	5.65	5.60
5.65	8.12	6.84	6.43	6.17	5.70	5.65
5.70	8.16	6.88	6.48	6.22	5.74	5.70
5.75	8.20	6.93	6.53	6.27	5.78	5.75
5.80	8.24	6.97	6.58	6.32	5.83	5.80
5.85	8.28	7.01	6.62	6.37	5.87	5.85
5.90	8.31	7.05	6.67	6.42	5.91	5.90
5.95	8.35	7.10	6.72	6.46	5.96	5.95
6.00	8.39	7.14	6.77	6.51	6.00	6.00

where

$$\epsilon = 1 + \delta + \sqrt{\delta^2 + 2\delta} \quad (19)$$

$$\delta = \frac{2}{\tan^2 \left[ (1 - \frac{b}{2B}) \pi \right]} \quad (20)$$

An example of the location is shown in figure 8. The location is a single-valued function of the constriction ratio (fig. 10 and table 6). It is always in a zone of nearly one-dimensional flow.

The approach reach friction losses are computed from equation 15 and 17.

$$h_{f(1-2)} = \frac{L_{av}(1-2)Q^2}{K_1 K_c} \quad (21)$$

where the controlling conveyance,  $K_c$ , at the downstream end of the approach reach is the smallest of the conveyances,  $K_3$ ,  $K_d$ , or  $K_q$ .

Friction losses between section d and section 2 and between section 2 and section 3 are computed using equations 15 and 16 where the length is the straight-line distance between sections. Therefore, the total friction loss between sections 1 and 3 is

$$h_{f(1-3)} = Q^2 \left[ \frac{L_{av}(1-d)}{K_1 K_c} + \frac{L_{av}(d-2)}{K_3 K_d} + \frac{L_{av}(2-3)}{K_3^2} \right] \quad (22)$$

#### Energy Losses in Flow Expansion Reach

In the flow expansion reach, the flow is assumed to be at natural elevation one-bridge-width downstream from section 3. Therefore, the area and conveyance of section 4 are computed at the natural elevation. The friction losses are estimated from equation 23 using the straight-line distance between sections,

$$h_{f(3-4)} = \frac{bQ^2}{K_c K_{4n}} \quad (23)$$

where the controlling conveyance,  $K_c$ , is the smaller of the conveyances  $K_d$  or  $K_3$ . The flow expansion losses are computed from an approximate solution of the momentum, energy, and continuity equations for an ideal expansion in open-channel flow (Henderson, 1966).

$$h_e = \frac{Q^2}{2gA_4^2} \left[ (2\beta_4 - \alpha_4) - 2\beta_3 \frac{A_4}{A_3} + \alpha_3 \left( \frac{A_4}{A_3} \right)^2 \right] \quad (24)$$

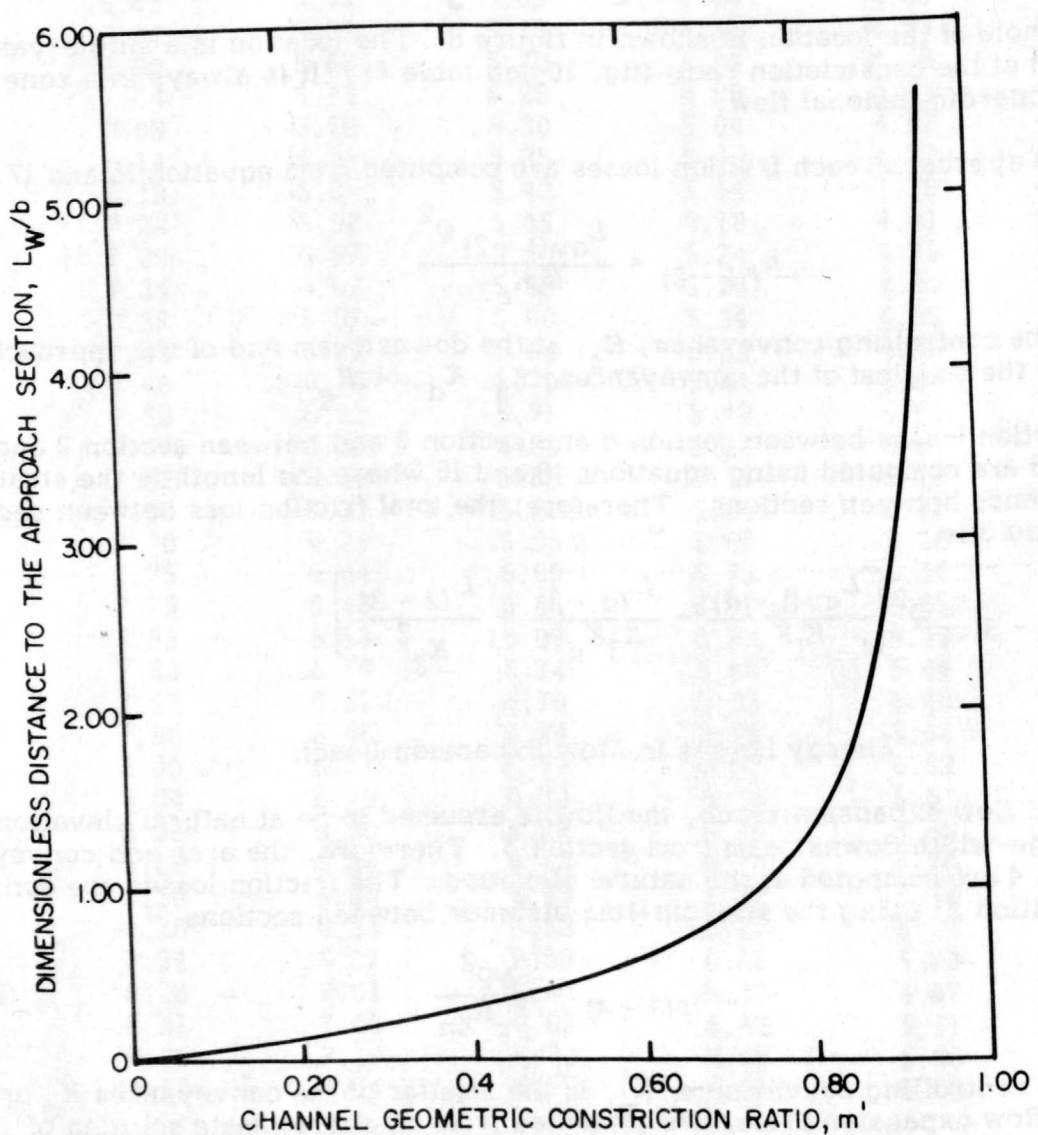


Figure 10.--Ratio of the distance to the approach section and the width of the constricted section as a function of the geometric constriction ratio.

Table 6.--Ratio of the distance to approach section and the width of the constricted section as a function of the geometric constriction ratio

$m'$	$L_w/b$									
	0	1	2	3	4	5	6	7	8	9
0.0	0.0	0.01	0.02	0.02	0.03	0.03	0.04	0.04	0.04	0.05
0.1	0.06	0.06	0.07	0.07	0.08	0.09	0.09	0.10	0.11	0.11
0.2	0.12	0.13	0.14	0.14	0.15	0.16	0.17	0.17	0.18	0.19
0.3	0.20	0.21	0.22	0.23	0.24	0.25	0.26	0.27	0.28	0.29
0.4	0.30	0.31	0.32	0.33	0.34	0.35	0.37	0.38	0.39	0.41
0.5	0.42	0.43	0.45	0.46	0.48	0.50	0.51	0.53	0.55	0.57
0.6	0.59	0.61	0.63	0.65	0.69	0.70	0.73	0.76	0.79	0.82
0.7	0.85	0.89	*0.92	0.96	1.01	1.05	1.10	1.16	1.21	1.28
0.8	1.35	1.42	1.51	1.60	1.71	1.83	1.96	2.12	2.30	2.52
0.9	2.78	3.09	3.48	3.99*	4.66	5.60	7.00	9.34	14.02	----

\*----\*Values of  $L_w/b$  (for  $m'$  between 0.72 and 0.93) that were used in this study.

where  $\beta$  and  $\alpha$  are the momentum and energy coefficients. The energy and momentum coefficients at section 4,  $\alpha_4$  and  $\beta_4$ , are computed from the conveyance distribution, and  $\alpha_3$  and  $\beta_3$  can be approximated as a function of the discharge coefficient,  $C$ . The discharge coefficient is computed by procedures outlined by Matthai (1967). The energy and momentum coefficients at section 3 can be approximated as follows:

$$\alpha_3 = \frac{1}{C^2} \quad (25)$$

$$\beta_3 = \frac{1}{C} \quad (26)$$

The total energy loss in the flow expansion reach is the sum of equations 20 and 21.

$$h_{L(3-4)} = h_{f(3-4)} + h_e \quad (27)$$

#### Proposed Method to Compute Backwater and Discharge

Backwater is the difference in the water-surface profiles for the natural and constricted conditions. The natural profile is computed using a standard step-backwater procedure (Chow, 1959), where the friction losses are

$$h_{f(i-j)n} = \frac{L(i-j)Q^2}{K_{in}K_{jn}} \quad (28)$$

The constricted profile is also computed using a standard step-backwater procedure where the friction losses are computed from equations 22 and 27. Both profiles use section 4 as a common starting point. The approach section is located using the data in figure 10 or table 6, and the average flow path needed in equation 22 is obtained from figure 9 or table 5.

The constricted water-surface profile is computed by iteration because the controlling conveyances are not known. The controlling conveyance,  $K_c$ , is computed at the natural water-surface elevation and used as the first estimate. Revised estimates of the controlling conveyances are determined at the computed constricted elevations and compared to the previous estimates. Successive estimates of the constricted profile are continued until the controlling conveyances agree within a preselected tolerance. With a tolerance criterion of  $K_c^{k-1} \approx 0.95K_c^k$ , convergence can be achieved in two or three iterations. The superscript is the iteration number. An example of the proposed method for computing backwater is included in the last section of this report.

Discharge can be computed from recovered high-water marks for wide, heavily vegetated channels. The Survey method (Matthai, 1967) is used except that the friction loss term in equation 1 is computed from equation 22 and the approach section is located using the data in figure 10 or table 6. The contracted water-surface elevation at section 3 is obtained by extrapolating the measured water-surface profile along the downstream side of the embankment to the intersection of the abutment and embankment for each side and averaging the values obtained.

## RESULTS

Backwater was computed by the proposed method developed in this study using the field data. When the constriction was relatively symmetric, the approach section was located as surveyed and the average flow path computed from table 5 based on this location. Since many of the bridges were constructed at natural valley constrictions, the backwater due to the natural constriction was computed and subtracted from the total backwater due to the natural constriction and highway encroachment.

For flood numbers 1, 4, 6 and 15, the constriction was judged to be geometrically eccentric ( $e' = \text{yes}$  in table 9) based on the position of the bridge. In these cases, the average flow path from table 5 was computed based on  $L_w/2b$ . The approach section was interpolated to the location given in table 6 for floods number 1 and 4. For flood number 6, it was necessary to sequentially compute the backwater caused by an abandoned roadfill downstream and then the backwater caused by the constriction. For convenience the approach section was used as surveyed, and the average flow path was computed based on that location. For flood number 15, an old roadfill upstream caused the constriction to be effectively eccentric. In this case, an approach section was interpolated at a location approximately two bridge widths upstream which is the correct location for computation by the Survey method. Again, for convenience, this section was also used for the proposed method.

The results are summarized in table 7 and figure 11. Deviations of the computed results from the measured data are reported in table 8 as mean percent error and standard deviation from the mean percent error. The backwater results are grouped in 0.5-ft (0.15-m) intervals of measured backwater. The mean error for the Survey method ranged from -20 to -45 percent, while the FHWA method ranged from -4 to -75 percent.

Care was taken to be objective in applying the Survey and FHWA methods. The variables needed to apply the methods were selected and the results recorded as computed. The errors in computing the natural elevation and the variation in high-water marks could be 0.5 ft (0.15 m) in some cases. Hence, measured backwater less than 0.5 ft (0.15 m) is not considered significant. Backwater computed by the Survey and FHWA methods between 0.5 and 1.0 ft was consistently lower than the measured. However, since the error varied up to -40 percent or -0.4 ft (0.12 m), the computed backwater approached the accuracy of the measured field data. For backwater greater than 1.0 ft, the errors were less significant and the values computed by the Survey and FHWA methods were decidedly low. The mean errors of +13 to -12 percent, achieved with the proposed method, are well within acceptable limits.

Table 7.--Summary of data for computing backwater by the proposed method

Flood no.	Q ft <sup>3</sup> /s	m <sup>1</sup>	b ft	C	h <sub>4</sub> ft	A <sub>4</sub> ft <sup>2</sup>	K <sub>4</sub> ft <sup>3</sup> /s	a <sub>4</sub>	L <sub>3-4</sub> ft	Measured			Computed			L <sub>2-3</sub> ft	Computed			L <sub>d</sub> ft
										h <sub>3</sub> ft	A <sub>3</sub> ft <sup>2</sup>	K <sub>3</sub> ft <sup>3</sup> /s	h <sub>3</sub> ft	A <sub>3</sub> ft <sup>2</sup>	K <sub>3</sub> ft <sup>3</sup> /s		h <sub>d</sub> ft	A <sub>d</sub> ft <sup>2</sup>	K <sub>d</sub> ft <sup>3</sup> /s	
1	1,780	0.80	222	0.73	27.04	1,640	25,000	1.00	110	27.57	1,000	27,400	27.40	950	26,100	48	---	---	---	---
2	2,250	0.72	242	0.81	23.93	2,910	68,900	1.23	370	24.47	1,220	88,900	25.40	1,200	89,700	46	---	---	---	---
3	4,150	0.73	247	0.81	25.41	4,920	123,200	1.14	370	26.22	1,620	147,400	26.10	1,590	142,700	45	---	---	---	---
4	5,600	0.79	464	0.86	31.30	5,140	134,400	1.18	180	31.39	2,360	182,000	31.60	2,470	194,800	41	32.00	3,720	120,000	210
5	1,550	0.81	149	0.71	26.79	1,700	42,900	1.41	140	26.86	670	50,500	27.00	690	52,300	37	---	---	---	---
6	2,000	0.76	246	0.73	27.94	2,950	66,000	1.00	890	29.41	970	59,300	29.27 <sup>a</sup>	940	55,780	34	---	---	---	---
7	6,600	0.79	250	0.73	30.64	5,880	187,200	1.00	890	32.40	1,740	151,000	32.55 <sup>a</sup>	1,780	154,700	31	---	---	---	---
8	1,900	0.82	200	0.72	31.25	1,360	27,500	1.01	210	32.13	630	33,900	32.20	660	30,400	39	---	---	---	---
9	4,600	0.84	200	0.73	33.10	3,150	77,900	1.05	210	33.93	1,040	62,500	33.90	1,020	62,250	33	---	---	---	---
10	12,100	0.88	158	0.76	369.51	5,340	291,300	1.77	101	369.47	1,320	155,300	369.00	1,243	140,500	28	---	---	---	---
11	16,100	0.92	178	0.83	363.80	11,350	576,200	2.15	451	364.80	2,010	263,100	363.90	1,830	228,000	64	---	---	---	---
12	12,500	0.81	486	0.75	310.00	9,474	411,000	2.74	1,060	311.56	3,950	617,000	311.60	3,950	617,000	32	311.70	4,020	276,900	60
13	17,900	0.81	493	0.75	310.99	11,270	528,000	2.41	1,060	312.30	4,320	709,100	312.80	4,570	772,900	30	312.90	4,620	338,400	60
14	3,800	0.89	240	0.81	198.30	9,180	168,700	1.40	1,050	199.54	1,310	194,200	199.30	1,250	194,200	34	199.40	1,060	138,800	150
15	10,200	0.75	546	0.87	353.45	12,800	463,600	4.40	1,365	354.14	4,480	569,200	354.20	4,520	587,700	46	354.20	4,130	243,700	150
16	8,100	0.88	546	0.89	352.94	10,700	392,000	4.80	1,365	353.46	4,100	515,500	353.70	4,240	531,000	49	353.70	3,810	218,300	150
17	25,000	0.92	397	0.72	305.00	19,900	810,000	2.25	595	305.40	4,750	710,200	305.60	4,880	730,200	34	---	---	---	---
18	31,500	0.93	400	0.72	305.44	21,900	1,109,100	2.15	595	305.78	4,970	750,430	305.90	5,000	760,700	34	---	---	---	---
19	31,000	0.92	399	0.71	305.77	23,500	1,069,900	1.81	595	305.84	4,890	755,600	306.20	5,130	791,600	34	---	---	---	---
20	25,600	0.87	336	0.95	282.74	12,750	741,200	2.47	520	283.60	4,450	914,800	283.50	4,410	903,700	41	283.90	5,120	708,800	150
21	29,500	0.87	336	0.93	283.28	14,590	865,600	2.34	520	283.90	4,560	948,800	284.00	4,600	960,300	41	284.50	5,360	760,200	150
22	3,500	0.80	497	0.69	349.90	5,200	114,200	1.24	1,440	352.12	2,050	163,800	351.70	1,840	142,800	55	---	---	---	---
23	4,900	0.82	496	0.69	350.00	5,480	123,500	1.22	1,440	352.50	2,240	184,100	352.50	2,240	184,100	55	---	---	---	---
24	4,200	0.93	112	0.70	31.79	6,740	155,600	1.03	520	32.35	835	86,500	32.40	840	87,300	26	---	---	---	---
25	1,500	0.87	108	0.79	28.00	1,280	32,500	1.09	200	28.45	400	27,000	28.60	420	28,800	42	---	---	---	---
26	4,740	0.88	150	0.81	39.20	7,740	336,600	3.42	320	39.50	2,040	269,250	39.40	2,020	266,300	74	---	---	---	---
27	5,500	0.77	205	0.75	86.13	2,240	109,200	2.50	610	87.51	1,400	144,900	87.70	1,440	151,700	47	---	---	---	---
28	9,500	0.77	210	0.74	87.77	3,380	210,200	2.62	610	88.51	1,610	180,900	89.00	1,720	200,200	42	---	---	---	---
29	14,200	0.89	266	0.86	320.25	7,710	357,100	3.39	260	320.99	2,880	520,400	321.20	2,940	534,000	40	321.30	2,710	304,700	110
30	17,000	0.90	266	0.86	321.25	9,470	460,250	3.15	260	321.88	3,120	581,700	322.10	3,180	597,500	38	322.30	3,060	359,500	110
31	6,400	0.79	518	0.75	14.70	8,100	195,300	1.04	880	15.54	2,980	237,000	16.00	3,240	268,600	40	---	---	---	---

<sup>a</sup>This event had additional backwater from an old roadfill downstream. The additional backwater at section 3 was determined to be 0.37 ft for the 12-21-72 event (6) and 0.65 ft for the 3-12-73 event (7).

Table 7.--Continued

Flood no.	$K_q$ ft <sup>3</sup> /s measured	$K_q$ ft <sup>3</sup> /s computed	Measured				Computed				$L_{1-2}$ ft	$L_{av}$ ft	$h_{1n}$ ft	$h_{3n}$ ft	$h_1^*$ ft measured	$h_1^*$ ft computed	$h_3^*$ ft measured	$h_3^*$ ft computed
			$h_1$ ft	$A_1$ ft <sup>2</sup>	$K_1$ ft <sup>3</sup> /s	$\alpha_1$	$h_1$ ft	$A_1$ ft <sup>2</sup>	$K_1$ ft <sup>3</sup> /s	$\alpha_1$								
1	36,200	37,000	28.86	3,300	77,500	1.05	28.80	3,230	75,900	1.05	600	770	28.27	27.38	0.59	0.53	0.19	0.02
2	37,500	37,500	25.02	3,160	88,700	1.05	25.00	3,140	87,900	1.05	260	320	24.56	24.24	0.46	0.44	0.23	1.16
3	59,000	59,100	26.87	4,790	147,360	1.05	26.90	4,820	171,400	1.05	260	325	26.19	25.87	0.68	0.71	0.35	0.23
4	111,500	132,400	33.37	7,700	231,000	1.10	33.50	8,450	282,500	1.06	1,190	1,530	32.96	31.61	0.41	0.54	-0.22	-0.01
5	26,800	26,600	27.62	2,290	57,000	1.15	27.60 <sup>b</sup>	2,280	56,300	1.17	170	230	27.22	26.97	0.40	0.38	-0.11	0.03
6	39,700	48,500	30.30	3,520	93,200	1.07	30.45 <sup>b</sup>	3,680	99,000	1.06	240	360	29.83	29.53	0.47	0.62	-0.12	-0.26
7	103,200	105,400	33.51	6,990	276,400	1.09	33.60 <sup>b</sup>	7,100	282,800	1.08	240	325	32.98	32.47	0.53	0.62	-0.07	0.08
8	27,400	25,700	33.13	3,320	93,500	1.04	33.00	3,170	87,200	1.05	270	360	32.44	31.92	0.69	0.56	0.21	0.28
9	55,000	50,600	35.60	6,260	213,800	1.03	35.30	5,890	194,100	1.03	270	375	34.24	33.65	1.36	1.06	0.28	0.25
10	230,900	221,000	371.92	9,290	1,116,400	1.29	371.80	9,030	1,066,000	1.29	160	265	370.31	370.18	1.61	1.49	-0.71	-1.18
11	376,600	324,500	367.15	17,350	1,717,200	1.57	366.10	14,930	1,368,000	1.57	254	470	364.07	363.64	3.08	2.03	1.16	0.26
12	153,500	149,800	313.11	16,980	778,760	1.11	313.00	16,700	759,400	1.10	526	715	311.84	310.90	1.27	1.16	0.66	0.70
13	192,100	204,400	314.10	19,570	982,800	1.12	314.40	20,400	1,047,800	1.12	526	720	312.94	312.00	1.16	1.46	0.30	0.80
14	37,200	35,700	200.50	9,130	179,400	1.08	200.50	9,130	179,400	1.08	256	429	199.40	198.90	1.10	1.10	0.64	0.40
15	271,300	271,300	355.60	11,000	509,400	2.22	355.60	11,000	509,400	2.22	1,089	1,395	354.50	354.10	1.10	1.10	0.04	0.10
16	208,900	209,000	354.46	14,270	483,700	2.90	354.50	14,400	492,200	2.86	689	1,080	353.96	353.56	0.50	0.54	-0.10	0.14
17	543,300	531,700	308.10	32,170	1,701,200	2.91	307.90	31,100	1,594,600	3.15	1,297	1,980	306.50	305.61	1.60	1.40	-0.21	-0.01
18	586,200	586,200	308.78	35,890	2,001,000	2.57	308.80	35,900	2,001,000	2.57	1,297	2,080	306.60	305.88	2.18	2.20	-0.10	0.02
19	572,900	591,000	308.58	35,820	1,917,900	2.64	308.90	36,400	2,044,000	2.53	1,297	1,980	307.18	306.32	1.40	1.72	-0.48	-0.12
20	466,200	455,600	285.30	20,670	974,000	2.81	285.10	20,000	936,100	2.85	348	555	283.95	283.25	1.35	1.15	0.35	0.25
21	503,500	498,100	286.00	22,890	1,117,100	2.66	285.90	22,600	1,096,100	2.68	348	555	284.58	283.92	1.42	1.32	-0.02	0.08
22	65,600	60,000	353.60	5,930	151,300	1.13	353.40	5,430	132,700	1.18	835	1,040	352.87	351.70	0.73	0.53	0.42	0.00
23	83,400	83,400	354.20	7,480	210,500	1.16	354.20	7,480	210,500	1.16	835	1,080	353.32	352.10	0.88	0.88	0.40	0.40
24	25,350	26,400	33.48	9,300	233,000	1.02	33.70	9,620	278,900	1.02	118	250	32.26	32.15	1.22	1.44	0.20	0.25
25	12,300	12,100	29.64	2,600	51,600	1.06	29.60	2,570	50,400	1.07	103	170	28.79	28.45	0.85	0.81	0.00	0.15
26	66,300	63,800	40.10	6,170	229,750	1.08	39.90	5,930	216,400	1.18	106	190	39.00	38.95	1.10	0.90	0.55	0.45
27	79,000	81,200	88.49	4,260	227,800	1.93	88.60	4,350	235,400	1.93	265	335	87.77	87.37	0.72	0.83	0.14	0.33
28	129,460	135,400	90.11	5,710	395,700	1.93	90.30	5,900	415,800	1.92	270	340	89.25	88.81	0.86	1.05	-0.30	0.19
29	135,000	134,000	323.90	17,300	639,200	1.18	323.70	17,700	689,000	1.14	518	770	321.92	320.80	1.98	1.78	0.19	0.40
30	157,600	157,600	324.66	19,300	755,000	1.15	324.60	19,300	755,000	1.15	518	790	322.58	321.70	2.08	2.02	0.18	0.46
31	100,000	108,800	16.60	11,810	327,300	1.08	16.80	12,300	348,900	1.08	520	695	15.87	15.45	0.73	0.93	0.09	0.55

<sup>b</sup>This event had additional backwater from an old roadfill downstream of the constriction. At section 1 it was determined to be 0.25 ft for the 12-21-71 event (6) and 0.60 ft for the 3-12-73 event (7).

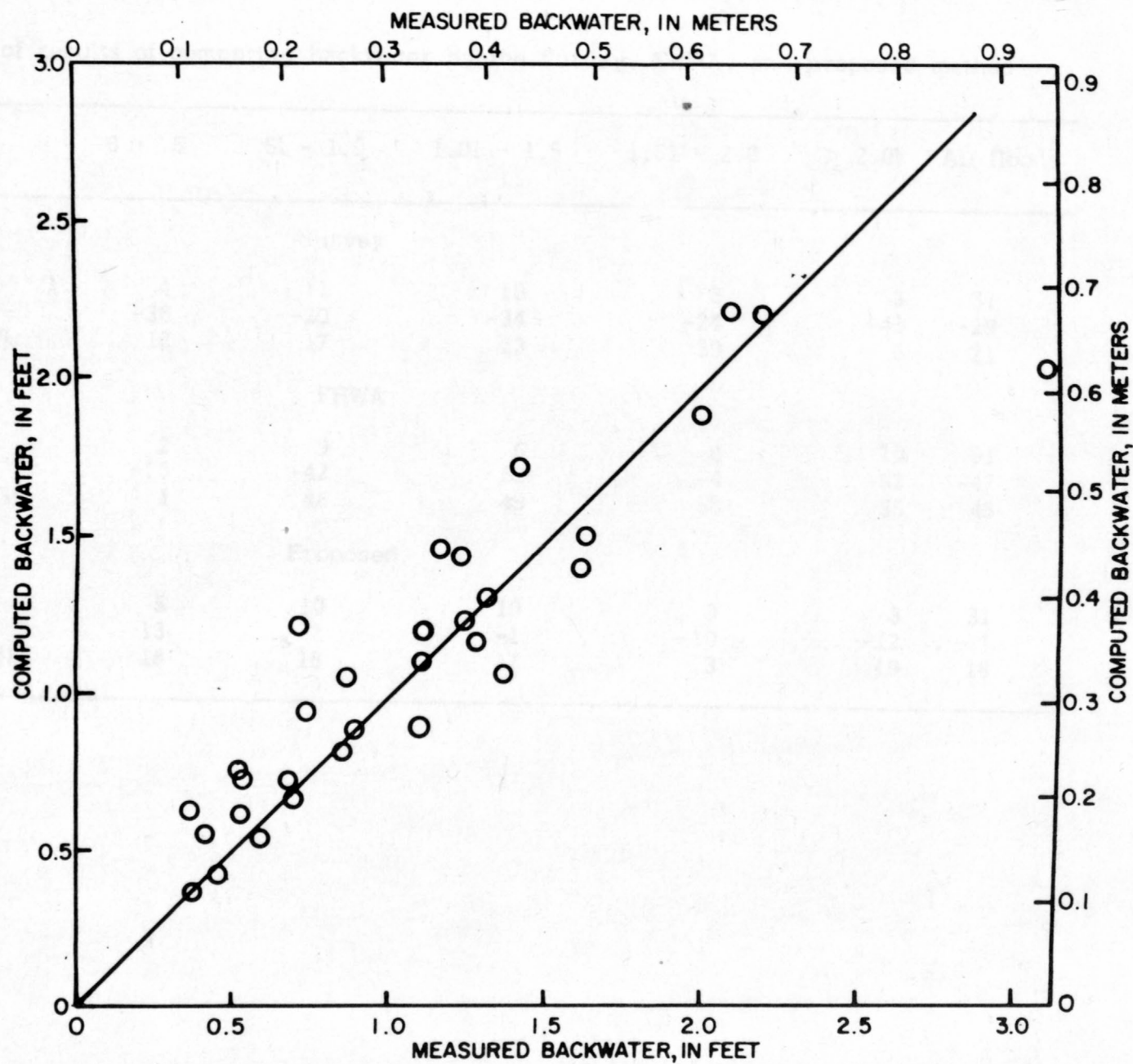


Figure 11.--Comparison of measured backwater to that computed by the proposed method.

Table 8.--Comparison of results of computing backwater by the Survey, FHWA, and proposed method

Measured $h_1^*$ , ft	0 - .5	.51 - 1.0	1.01 - 1.5	1.51 - 2.0	> 2.01	All floods
Survey						
Number of floods	4	11	10	3	3	31
Mean error (%)	-36	-20	-34	-24	-45	-29
Standard deviation (%)	12	17	23	39	6	21
FHWA						
Number of floods	2	9	6	4	10	31
Mean error (%)	-75	-42	-63	-4	-52	-47
Standard deviation (%)	1	46	49	58	35	45
Proposed						
Number of floods	5	10	10	3	3	31
Mean error (%)	13	2	-1	-10	-12	1
Standard deviation (%)	18	18	17	3	19	18

In the proposed method, the average water-surface elevation was computed at section 3. As may be seen from the results in table 7, the computed elevation is higher than that measured for 65 percent of the floods, by an average of 0.07 ft (0.92 m). The measured water-surface elevation,  $h_3$ , was obtained by extrapolating the measured water-surface profile along the downstream side of the embankment to the intersection of the abutment and embankment. This procedure results in a value of  $h_3$ , which was less than the average by a small amount. The average value of 0.07 ft (0.02 m) seems reasonable.

The results of computing discharge using the proposed method are shown in table 9 and figure 12. The mean error for the Survey method is 21 percent with a standard deviation of 14 percent. Using the proposed modification to the Survey method, the mean error is reduced to 3 percent with a standard deviation of 9 percent.

In the previous comparisons of measured and computed backwater and discharge, the approach section location was used as surveyed and the average flow path selected from table 6 based on the surveyed location. In the following analysis, an attempt was made to evaluate the errors due to approach-section location. Even though the field data were collected according to Survey standards, the approach section was surveyed within 5 percent of one-bridge-opening width at only seven sites. An approach section at the proposed location was not available for any site.

The percentage error in computed backwater and discharge is plotted on figures 13 and 14 as a function of the ratio of the measured and proposed distances to the approach section. The percentage errors for the computed backwater and discharge are tabulated in table 10. The open points are backwater and discharge computed by Survey methods, while the closed points are backwater and discharge computed by proposed methods. In each case the data were used as surveyed except for flood numbers 1, 4, 6, and 15 as noted above. A line connects pairs of points for the same flood. Circles represent sites where  $L_w$  is within  $\pm 25$  percent of one-bridge-opening width,  $b$ . The triangles include all other sites.

Discharge data for 11 additional floods were also plotted in figure 14 and summarized in table 11. These data include sites used by Liu and others (1957) for field verification. Data for other sites were obtained from Survey files (J. Davidian, written commun., 1975). Since these sites were used to verify the procedures discussed by Matthai (1967), they are called the verification sites.

If the distance to the approach section is not important, the percent error should be independent of the distance ratio. The mean errors and standard deviations were computed and are summarized in table 12 for various groups of sites.

The mean percent errors in computing discharge for the verification sites were not significantly affected by the average flow path, because the contraction ratio,  $m'$ , was in the range where  $L_{gy}$  was nearly equal to  $L_w$  for these sites. Also, the accuracy of the computed discharge is independent of the approach section location for the verification sites.

Table 9.--Summary of data for computing discharge by the proposed method

Flood no.	$\Delta h$ ft	$b$ ft	$m'$	$e'$	$L_{1-2}$ ft	$L_{av}$ ft	$C$	$L$ ft	$a_1$	$A_1$ ft <sup>2</sup>	$K_1$ ft <sup>3</sup> /s	$L_d$ ft	$K_d$ ft	$A_3$ ft <sup>2</sup>	$K_3$ ft <sup>3</sup> /s	$K_q$ ft <sup>3</sup> /s	$Q$ ft <sup>3</sup> /s measured	$Q$ ft <sup>3</sup> /s computed	Percent difference
1	1.29	222	0.80	Yes	600	770	0.73	48	1.05	3,300	77,500	---	---	1,000	27,400	36,200	1,780	1,680	-6
2	0.55	242	0.72	No	260	320	0.81	46	1.05	3,160	88,700	---	---	1,220	88,900	37,500	2,250	2,170	-4
3	0.65	247	0.73	No	260	325	0.81	45	1.05	4,790	147,360	---	---	1,620	147,400	59,000	4,150	3,690	-11
4	1.98	464	0.79	Yes	1,190	1,530	0.86	41	1.10	7,700	231,000	210	137,500	2,360	182,000	111,500	5,600	5,230	-7
5	0.76	149	0.81	No	170	230	0.71	37	1.15	2,290	57,000	---	---	670	50,500	26,800	1,550	1,810	+17
6	0.89	246	0.76	Yes	240	360	0.73	34	1.07	3,520	93,200	---	---	970	59,300	39,700	2,000	2,550	+28
7	1.11	250	0.79	No	240	325	0.73	31	1.09	6,990	276,400	---	---	1,740	151,000	103,200	6,600	7,090	+7
8	1.00	200	0.82	No	270	360	0.72	39	1.04	3,320	93,500	---	---	630	33,900	27,400	1,900	2,000	5
9	1.67	200	0.84	No	270	375	0.73	33	1.03	6,260	213,800	---	---	1,040	62,500	55,000	4,600	5,000	9
10	2.45	158	0.88	No	160	265	0.76	28	1.29	9,290	1,116,400	---	---	1,320	155,300	230,900	12,100	11,700	-3
11	2.35	178	0.92	No	254	470	0.83	64	1.57	17,350	1,717,200	---	---	2,010	263,100	376,600	16,100	17,700	+10
12	1.55	486	0.81	No	526	715	0.75	32	1.11	16,980	778,760	60	301,900	3,950	617,000	153,500	12,500	13,800	+10
13	1.80	493	0.81	No	526	720	0.75	30	1.12	19,570	982,800	60	322,500	4,320	709,100	192,100	17,900	18,200	+2
14	0.96	240	0.89	No	256	429	0.81	34	1.08	9,130	179,400	150	159,800	1,310	194,200	37,200	3,800	3,390	-11
15	1.46	546	0.75	Yes	1,089	1,395	0.87	46	2.22	11,000	509,400	150	269,900	4,480	569,200	271,300	10,200	11,000	8
16	1.00	546	0.88	No	689	1,080	0.89	49	2.90	14,270	483,700	150	228,600	4,100	515,500	208,900	8,100	8,700	7
17	2.66	397	0.92	No	1,297	1,980	0.72	34	2.91	32,170	1,701,200	---	---	4,750	710,200	543,300	25,000	27,600	10
18	2.97	400	0.93	No	1,297	2,080	0.72	34	2.57	35,890	2,001,000	---	---	4,970	750,430	586,200	31,500	31,400	0
19	2.74	399	0.92	No	1,297	1,980	0.71	34	2.64	34,820	1,917,900	---	---	4,890	755,600	572,900	31,000	30,000	-3
20	1.70	336	0.87	No	348	555	0.95	41	2.81	20,670	974,000	150	742,900	4,450	914,800	466,200	25,600	27,400	7
21	2.10	336	0.87	No	348	555	0.93	41	2.66	22,890	1,117,100	150	777,600	4,560	948,800	503,500	29,500	32,200	9
22	1.48	497	0.80	No	835	1,040	0.69	55	1.13	5,930	151,300	---	---	2,050	163,800	65,600	3,500	3,600	3
23	1.70	496	0.82	No	835	1,080	0.69	55	1.16	7,480	210,500	---	---	2,240	184,100	83,400	4,900	4,950	1
24	1.13	112	0.93	No	118	250	0.70	26	1.02	9,300	233,000	---	---	835	86,500	25,350	4,200	3,520	-16
25	1.19	108	0.87	No	103	170	0.79	42	1.06	2,600	51,600	---	---	400	27,000	12,300	1,500	1,580	5
26	0.60	150	0.88	No	106	190	0.81	74	1.08	6,170	229,750	---	---	2,040	269,250	66,300	4,740	5,650	+19
27	0.98	205	0.77	No	265	335	0.75	47	1.93	4,260	227,800	---	---	1,400	144,900	79,000	5,500	5,430	-1
28	1.60	210	0.77	No	270	340	0.74	42	1.93	5,710	395,700	---	---	1,610	180,900	129,460	9,500	9,440	-1
29	2.91	266	0.89	No	518	770	0.86	40	1.18	17,300	639,200	110	342,600	2,880	520,400	135,000	14,200	15,500	9
30	2.78	266	0.90	No	518	790	0.86	38	1.15	19,300	755,000	110	376,900	3,120	581,700	157,600	17,000	17,200	1
31	1.06	518	0.79	No	520	695	0.75	40	1.08	11,810	327,300	---	---	2,980	237,000	100,000	6,400	6,520	+2

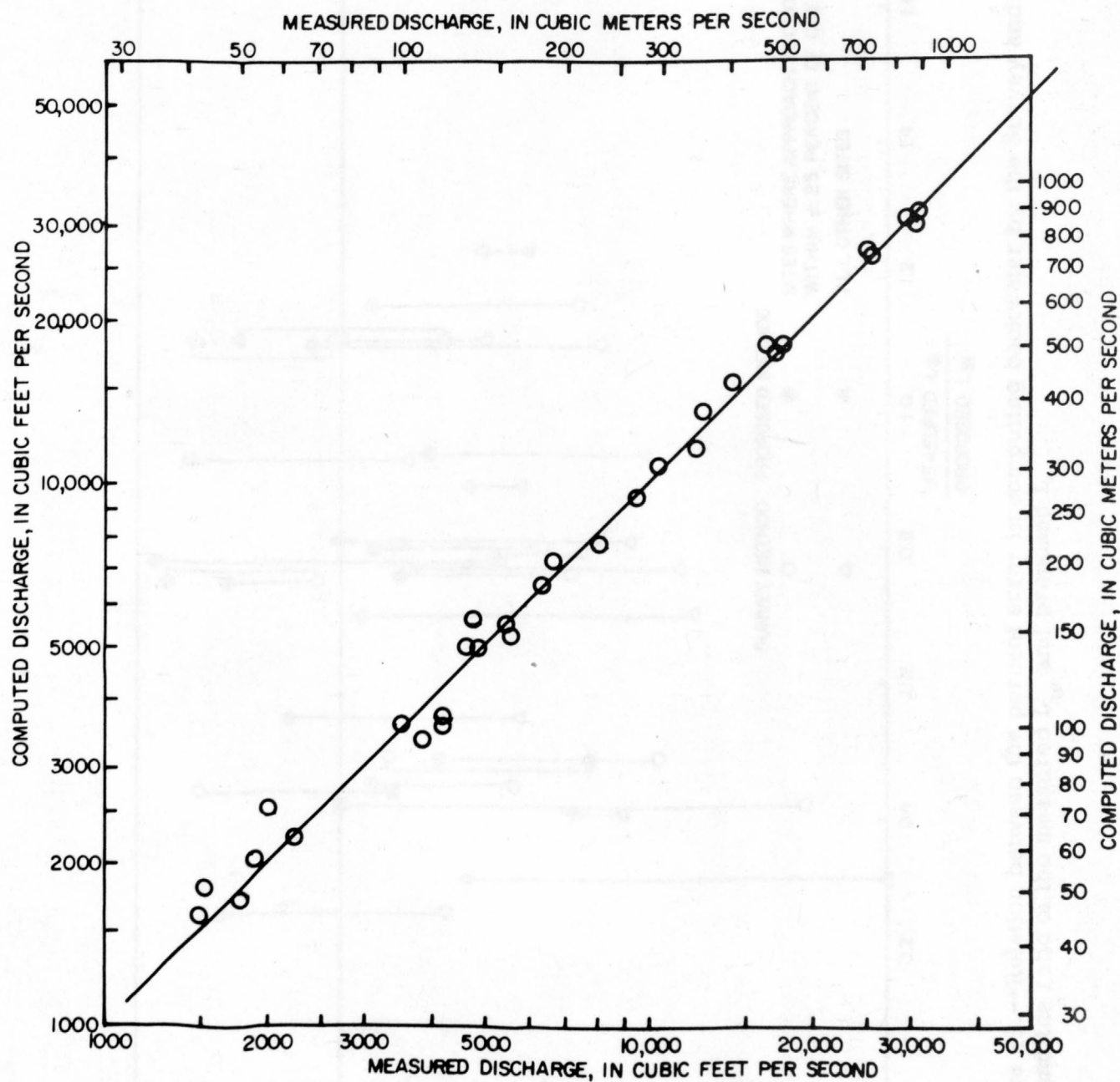


Figure 12.--Comparison of measured discharge to that computed by the proposed method.

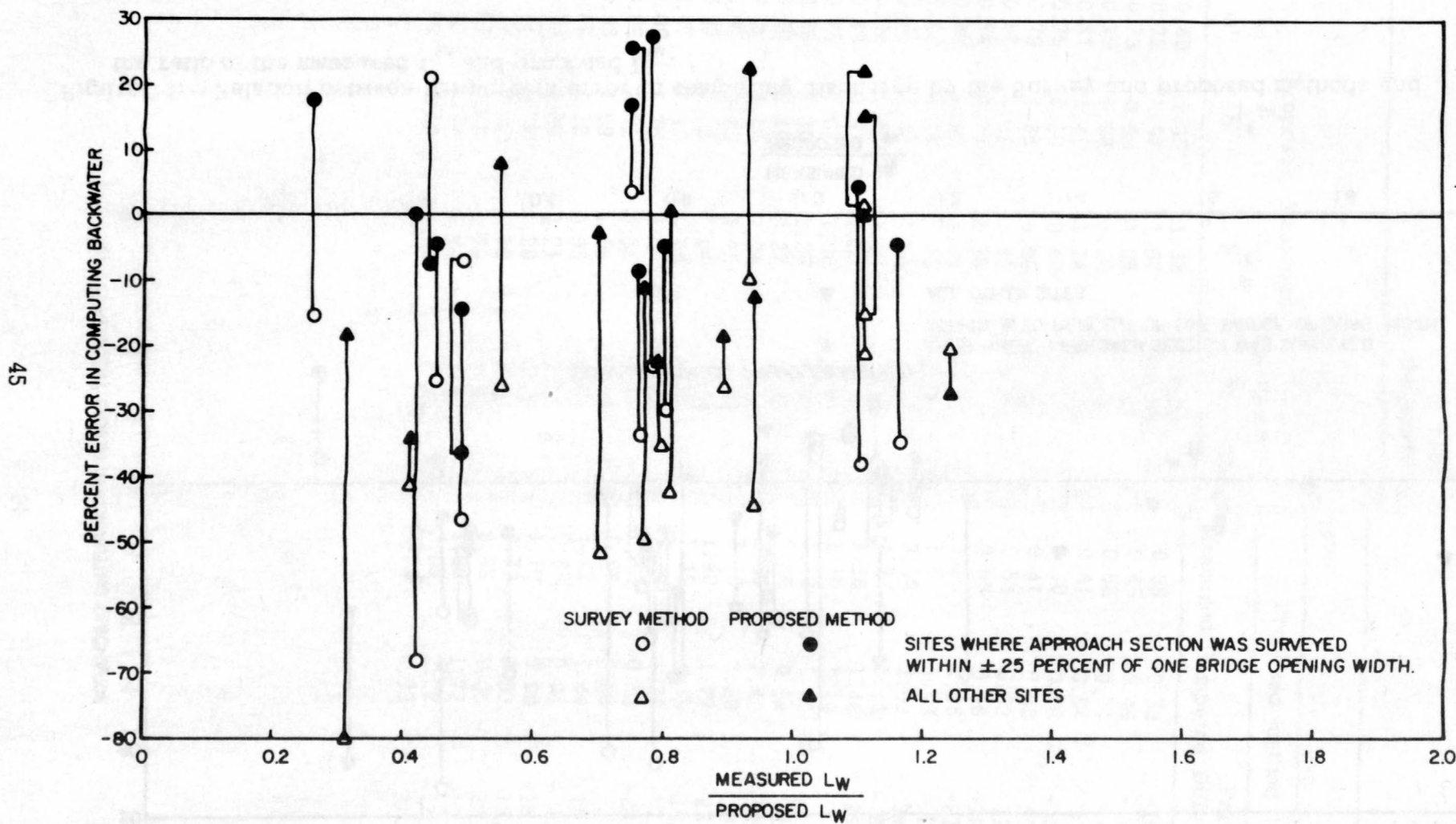


Figure 13.--Relation between the percent error in computing backwater by the Survey and proposed methods and the ratio of the measured  $L_w$  and proposed  $L_w$ .

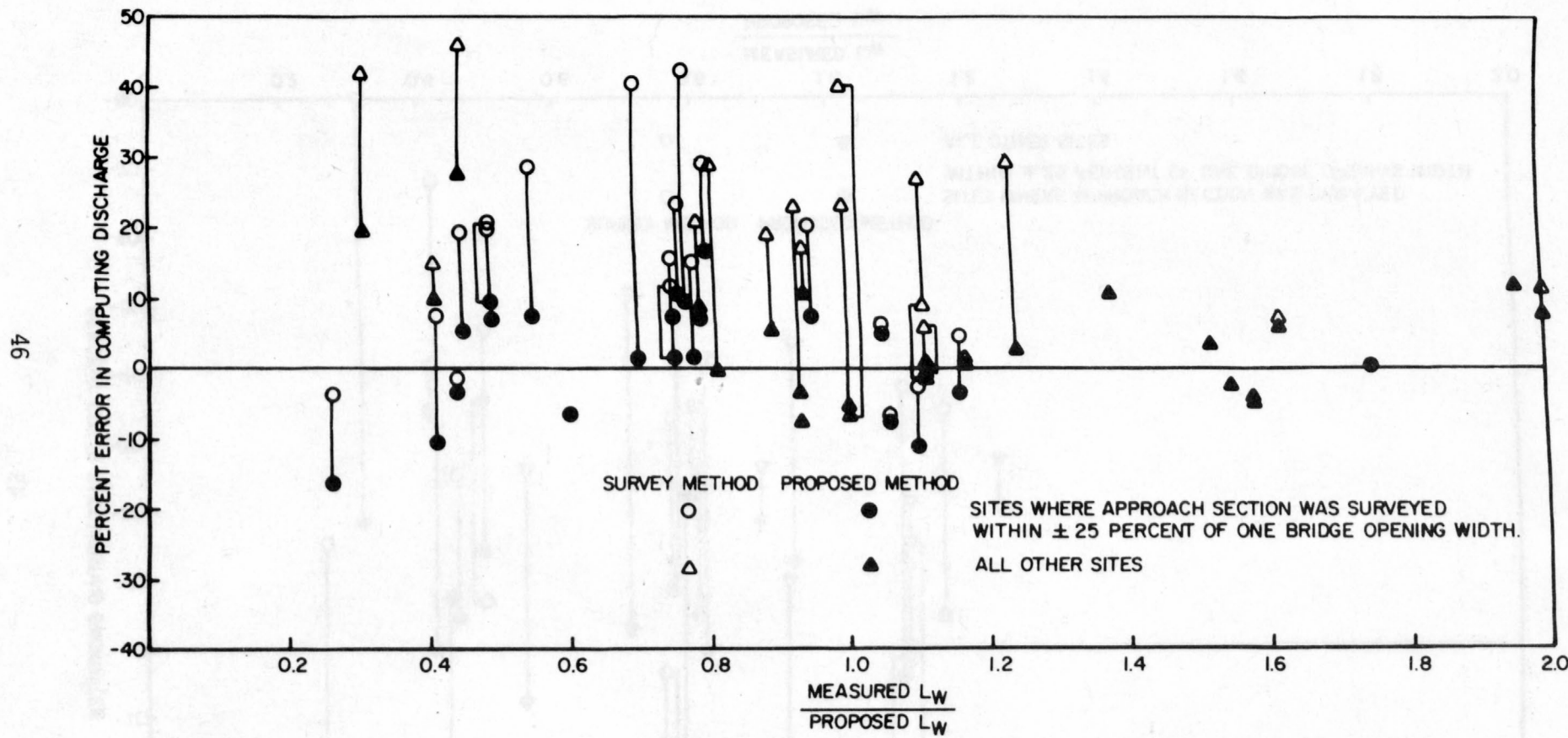


Figure 14.--Relation between the percent error in computing discharge by the Survey and proposed methods and the ratio of the measured  $L_w$  and proposed  $L_w$ .

Table 10.--Summary of data for evaluating the effect of distance to the approach section on the accuracy of the computed backwater and discharge

Flood no.	b (ft)	m'	Proposed $\frac{L_w}{b}$	Measured $\frac{L_w}{b}$	Discharge			Discharge			Backwater					
					Survey method		Proposed method		Survey method		Proposed method		Survey method		Proposed method	
					Measured $L_w$	Percent Difference	Measured	Percent Difference	Measured	Percent Difference	Measured	Percent Difference	Measured	Percent Difference	Measured	Percent Difference
1	222	0.80	1.35	1.35	1.00	1,780	2,200	23.6	1,680	-5.6	0.64	0.40	-37.5	0.59	0.53	-10.2
2	242	0.72	0.92	1.07	0.86	2,250	2,360	4.9	2,170	-3.6	0.46	0.30	-34.8	0.46	0.44	-4.3
3	247	0.73	0.96	1.05	0.91	4,150	4,030	-2.9	3,690	-11.1	0.68	0.42	-38.2	0.68	0.71	4.4
4	464	0.79	1.28	1.28	1.00	5,600	7,850	40.2	5,230	-6.6	0.69	0.51	-28.1	0.41	0.54	31.7
5	149	0.81	1.42	1.14	1.25	1,550	2,000	29.0	1,810	16.8	0.40	0.28	-30.0	0.40	0.38	-5.0
6	246	0.76	1.10	0.49	2.24	2,000	2,920	46.0	2,550	27.5	0.47	0.26	-44.7	0.47	0.62	31.9
7	250	0.79	1.28	0.96	1.33	6,600	7,630	15.6	7,090	7.4	0.53	0.55	3.8	0.53	0.62	17.0
8	200	0.82	1.51	1.35	1.12	1,900	2,270	19.5	2,000	5.3	0.69	0.51	-26.1	0.69	0.56	-18.8
9	200	0.84	1.71	1.35	1.27	4,600	5,580	21.3	5,000	8.7	1.36	0.88	-35.3	1.36	1.06	-22.1
10	158	0.88	2.30	1.01	2.27	12,100	11,900	-1.7	11,700	-3.3	1.61	1.95	21.1	1.61	1.49	-7.5
11	178	0.92	3.48	1.43	2.44	16,100	18,500	14.9	17,700	9.9	3.08	1.81	-41.2	3.08	2.03	-34.1
12	486	0.81	1.42	1.08	1.31	12,500	15,400	23.2	13,800	10.4	1.27	0.84	-33.9	1.27	1.16	-8.7
13	493	0.81	1.42	1.07	1.33	17,900	20,000	11.7	18,200	1.7	1.16	1.80	3.4	1.16	1.46	25.9
14	240	0.89	2.52	1.07	2.36	3,800	4,080	7.4	3,390	-10.8	1.10	0.70	-68.1	1.10	1.10	0
15	546	0.75	1.05	1.00	1.05	10,200	12,250	80.1	11,000	7.8	1.10	0.56	-49.1	1.10	1.10	0
16	546	0.88	2.30	1.26	1.82	8,100	10,400	28.4	8,700	7.4	0.50	0.37	-26.0	0.50	0.54	8.0
17	397	0.92	3.48	3.27	1.07	25,000	35,600	42.4	27,600	10.4	1.60	0.89	-44.4	1.60	1.40	-12.5
18	400	0.93	3.99	3.24	1.23	31,500	40,500	28.6	31,400	-0.3	2.18	1.25	-42.7	2.18	2.20	0.9
19	399	0.92	3.48	3.25	1.07	31,000	38,200	23.2	30,000	-3.2	1.40	1.26	-10.0	1.40	1.72	22.9
20	336	0.87	2.12	1.04	2.05	25,600	30,700	19.9	27,400	7.0	1.35	0.72	-46.7	1.35	1.15	-14.8
21	336	0.87	2.12	1.04	2.05	29,500	35,600	20.7	32,200	9.2	1.42	0.90	-36.6	1.42	1.32	-7.0
22	497	0.80	1.35	1.68	0.80	3,500	4,500	28.6	3,600	2.9	0.73	0.58	-20.5	0.73	0.53	-27.4
23	496	0.82	1.51	1.68	0.90	4,900	6,240	27.3	4,950	1.0	0.98	0.69	-21.6	0.98	0.88	0
24	112	0.93	3.99	1.05	3.79	4,200	4,050	-3.6	3,520	-16.2	1.22	1.03	-15.6	1.22	1.44	18.0
25	108	0.87	2.12	0.95	2.22	1,500	1,790	19.3	1,580	5.3	0.95	0.63	-25.9	0.85	0.81	-4.7
26	150	0.88	2.30	0.71	3.25	4,740	6,730	42.0	5,650	19.2	1.10	0.22	-80.0	1.10	0.90	-18.2
27	205	0.77	1.16	1.29	0.90	5,500	6,000	9.1	5,430	-1.3	0.72	0.61	-15.3	0.72	0.83	15.3
28	210	0.77	1.16	1.29	0.90	9,500	10,100	6.3	9,440	-0.6	0.86	1.04	20.9	0.86	1.05	22.1
29	266	0.89	2.52	1.95	1.29	14,200	20,200	42.3	15,500	9.2	1.89	0.95	-49.7	1.98	1.78	-10.1
30	266	0.90	2.78	1.95	1.43	17,000	23,900	40.6	17,200	1.2	2.32	1.12	-51.7	2.08	2.02	-2.9
31	518	0.79	1.28	1.00	1.28	6,400	7,360	15.0	6,520	1.9	0.73	0.56	-23.3	0.73	0.93	27.4

Table 11.--Summary of data from the verification files for evaluating the effect of distance to the approach section on the accuracy of computed backwater and discharge

Site	Date	b (ft)	m'	Proposed			Measured $L_w$	Measured $L_w$	Discharge			
				$\frac{L_w}{b}$	$\frac{L_w}{b}$	Measured			Survey Method		Proposed Method	
				Percent error	Percent error	Computed			Percent error	Computed	Percent error	Computed
Bond Brook at Dunham Basin, N.Y.	12-31-48	20	0.95	1.05	1.70	0.62	1,370	1,450	5.8	1,470	7.3	
Short Creek near Albertville, Ala.	11-28-48	86	0.28	0.18	0.91	0.20	12,000	11,200	-6.7	11,200	-6.7	
Big Turtle River above Rice Lakes, Minn.	06-05-50	25	0.79	1.28	1.00	1.28	326	350	7.4	350	7.4	
Neosho River near Burlington, Kan.	04-24-44	900	0.25	0.16	0.22	0.73	85,000	94,300	10.9	94,300	10.9	
McAlpine Creek at Sardis Road near Charlotte, N.C.	01-06-62	99	0.74	1.01	1.60	0.63	3,900	3,710	-4.9	3,740	-4.1	
Little River	02-01-57	232	0.64	0.69	1.35	0.51	19,000	21,200	11.6	21,200	11.6	
Oneida Creek at Oneida, N.Y.	03-28-50	75	0.46	0.37	1.33	0.28	7,900	7,900	1.3	7,900	1.3	
Wild Rice River near Twin Valley, Minn.	05-09-50	60	0.33	0.23	0.72	0.32	3,390	3,730	10.0	3,730	10.0	
Crooked Creek near Richmond, Mo.	07-06-51	230	0.74	1.01	1.06	0.95	18,000	15,900	5.0	19,150	6.4	
Elk River	05-15-46	356	0.64	0.69	1.21	0.57	49,900	49,930	0.1	49,930	0.1	
Kayderosseras Creek near West Milton, N.Y.	04-02-52	43	0.46	0.37	1.47	0.25	1,450	1,460	0.7	1,460	0.7	
Kayderosseras Creek near West Milton, N.Y.	04-04-52	43	0.37	0.92	1.40	0.66	774	800	3.4	800	3.4	
Kayderosseras Creek near West Milton, N.Y.	04-06-52	43	0.57	0.96	1.49	0.64	2,620	2,550	-2.7	2,550	-2.7	
Kayderosseras Creek near West Milton, N.Y.	06-01-52	43	0.43	0.33	1.47	0.22	1,320	1,210	-8.3	1,210	-8.3	
Kayderosseras Creek near West Milton, N.Y.	12-31-48	84	0.66	0.73	0.68	1.07	4,840	4,015	-7.5	4,015	-7.5	
Cypress Creek near Buna, Tex.	04-23-51	31	0.85	1.83	1.10	1.66	1,280	1,200	-6.3	1,200	-6.3	
Little Turtle River above Rice Lakes, Minn.	06-05-50	21	0.70	0.85	1.71	0.50	216	233	7.9	240	11.1	
Johnson Creek near Sycamore, Ore.	01-22-54	24	0.76	1.10	1.17	0.94	1,600	1,475	-7.8	1,490	-6.9	
Johnson Creek near Sycamore, Ore.	11-24-60	24	0.84	1.71	2.00	0.86	2,010	2,018	0.4	2,035	1.2	

Table 12.--Percent errors in computing backwater and discharge  
as a function of approach section location

Sample	Friction loss length	Discharge				Backwater			
		Project sites		Verification sites		Data		Project sites	
		Mean	Standard deviation	Mean	Standard deviation	Mean	Standard deviation	Mean	Standard deviation
Sites where measured $L_w$ is within $\pm$ 25 percent of one bridge opening width	$L_w$	12.8	10.4	-1.0	6.7	8.6	11.3	-26.7	23.6
	$L_{av}$	1.6	9.5	-1.4	6.5	0.7	8.6	2.9	13.6
	Number of sites	14		6		20		14	
Sites where measured $L_w$ is within $\pm$ 25 percent of proposed $L_w$	$L_w$	23.2	12.5	Insufficient data		18.5	15.1	-30.6	19.1
	$L_{av}$	3.6	7.8			2.7	7.7	0.4	17.6
	Number of sites	20		5		20		20	
Sites where measured $L_w$ is greater or equal to the proposed $L_w$	$L_w$	17.1	14.9	1.7	6.6	6.8	12.3	-21.6	19.2
	$L_{av}$	-3.1	4.6	2.2	6.8	0.43	6.6	4.0	18.9
	Number of sites	8		16		24		8	
Sites where measured $L_w$ is less than proposed $L_w$	$L_w$	22.9	13.4	Insufficient data		20.0	15.2	-32.7	23.0
	$L_{av}$	5.8	9.3			4.9	9.4	-0.6	17.4
	Number of sites	23		3		26		23	

Table 12.--Continued

Sample	Friction loss length	Discharge				Backwater				
		Project sites		Verification sites		Data		Project sites		
		Mean	Standard deviation	Mean	Standard deviation	Mean	Standard deviation	Mean	Standard deviation	
All sites in a data set	$L_w$	21.4	13.8	1.5	7.0	13.8	15.1	-29.9	22.3	
	$L_{av}$	3.5	9.1	1.1	6.8	2.6	8.3	0.6	17.6	
	Number of sites	31		19		50		31		
5	Sites where measured $L_w$ was less than half of the proposed $L_w$	$L_w$	18.3	17.1	No data		18.3	17.1	-38.6	31.4
		$L_{av}$	5.3	13.8			5.3	13.8	-4.0	19.5
		Number of sites	9		0		9	9		
5	Sites where measured $L_w$ is greater than half of the proposed $L_w$	$L_w$	22.6	12.4	1.5	7.0	12.9	14.7	-23.3	-26.0
		$L_{av}$	2.7	6.7	1.1	6.8	2.0	6.7	2.4	16.9
		Number of sites	22		19		41		22	

For the project sites, the largest reduction in error in computing backwater and discharge resulted from the use of  $L_{qv}$  in the friction loss term. At 14 sites where the measured  $L_w$  is within  $\pm 25$  percent of one  $b$  width, the mean error was reduced from 12.8 to 1.6 percent. At 20 sites where measured  $L_w$  is within  $\pm 25$  percent of the proposed  $L_w$ , the mean error was reduced from 23.2 to 3.6 percent. Seven sites were common to both groups. The mean error was reduced from 21.4 to 3.5 for all the sites taken together. The measured  $L_w$  ranged between 0.49 to 3.27  $b$  widths and between 0.26 and 1.24 of the proposed  $L_w$ . Therefore, satisfactory answers were obtained with the approach cross section located either at one  $b$  width or at the proposed location.

The results were about the same for project sites where the measured  $L_w$  is greater than the proposed  $L_w$  (17.1 to -3.1 percent) and where the measured  $L_w$  was less than the proposed  $L_w$  (22.9 to 5.8 percent). The slightly higher residual error, 5.8 percent, could be caused by the measured  $L_w$  being less than the proposed  $L_w$ . However, the data do not prove it.

At nine sites where the measured  $L_w$  is less than 0.5 of the proposed  $L_w$ , the error was reduced from 18.3 to 5.3 percent. Where the measured  $L_w$  is greater than 0.5 of the proposed  $L_w$ , the error was reduced from 22.6 to 2.7 percent. However, the standard deviation was significantly higher, 13.8 compared to 6.7 percent, at sites where the measured  $L_w$  was less than 0.5 of the proposed  $L_w$ . These comparisons, based on data from nine floods, suggest that an approach section could be surveyed too close to the bridge.

The distance to the approach section computed from equation 18 is theoretically correct because the flow at that distance is nearly one dimensional. However the available field data indicate that distances ranging from one-half to two times the proposed value work as well, as long as the average flow path is used in computing friction loss in the approach reach.

## CONCLUSIONS

Data were collected at 20 single opening sites for 31 floods. Flood-plain width varied from 4 to 14 times the bridge opening width. The recurrence intervals of peak discharge ranged from a 2-year flood to greater than the 100-year flood, with a median interval of 6 years. Measured backwater ranged from 0.39 to 3.16 ft (0.12 to 0.96 m). Backwater computed by the currently used standard Survey method averaged 29 percent less than that measured, and the value computed by the FHWA method averaged 47 percent less than that measured. Discharge computed by the Survey method averaged 21 percent more than that measured. Analysis of the data showed that the flood-plain widths and Manning's roughness coefficients are larger than those used to develop the currently used standard methods and the accurate computation of backwater and discharge depends on improving the method of computing the energy loss.

With the proposed method for computing backwater and discharge, the contracted and natural watersurface profiles were computed using standard step-backwater procedures. The difference between the profiles was defined as backwater. The energy loss terms in the step-backwater procedure were computed as the product of the geometric mean of the energy slopes and the representative flow distance between the ends of the reach. An estimate of the average flow path was derived from potential flow theory for the approach reach while an empirical method based on the straight-line distance between the bridge and a valley cross section one-bridge-opening width downstream was developed for the flow expansion reach. The mean error using the proposed method for computing backwater was 1 percent. The mean error using the proposed method for computing discharge was 3 percent.

## FUTURE WORK

The data were collected and the proposed method was developed and applied to single opening sites. The method developed here could be extended to multiple opening sites. To do this, additional data of the type collected in this study would be required for about 20 flood events preferably at 20 sites. More detailed high water information would be needed upstream of the bridge to estimate the flow split between bridges, but fewer valley cross sections would be required.

Engineering judgment was used to determine whether a constriction was eccentric. Furthermore, a constriction was considered to be either symmetric or fully eccentric. Preliminary computations indicate that it is theoretically feasible to determine the average flow path for eccentric constrictions using a Schwartz-Christoffel transformation.

The function describing the friction loss in the expansion reach is empirical, but apparently successful. The flow redistribution mechanism is complicated by the roughness downstream of the bridge. Additional laboratory studies into the nature of the rate at which energy is expended and flow redistributed would be worthwhile. It is difficult to collect the field data with the detail and control required to evaluate this process.

The data collected in this study could be used to evaluate  $n$  values on heavily vegetated flood plains. The reach downstream of the bridge could be used as an  $n$ -verification reach. The principal deficiency in the data is the lack of knowledge of the flow distribution. However, a careful comparative study between sites should overcome most of the problems. Verified  $n$  values and representative pictures would be obtained in such a study.

## EXAMPLE OF BACKWATER CALCULATIONS USING PROPOSED METHOD

A highway crossing of Example Creek is proposed. A plan of the reach and a typical cross section (the approach section) is shown in figure 15. The design discharge for the bridge crossing Example Creek is  $6,400 \text{ ft}^3/\text{s}$ . The natural stage at cross section 4,  $h_{4n}$ , is 14.5 ft. The spill-through abutments and the

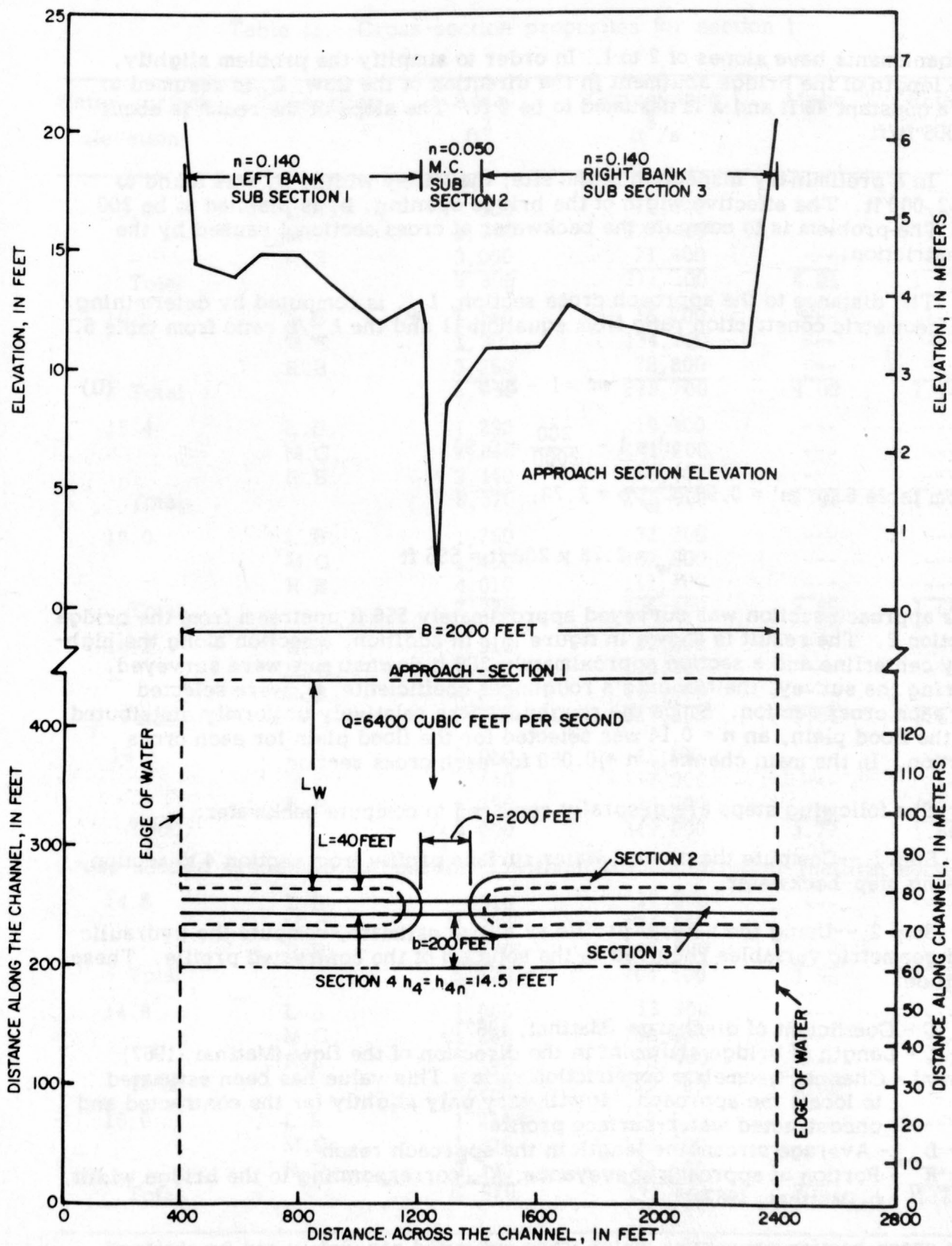


Figure 15.--Plan and approach cross section of Example Creek.

embankments have slopes of 2 to 1. In order to simplify the problem slightly, the length of the bridge abutment in the direction of the flow,  $L$ , is assumed to be a constant 40 ft and  $x$  is assumed to be 0 ft. The slope of the reach is about .0006 ft/ft.

In a preliminary inspection of the site, the valley width,  $B$ , was found to be 2,000 ft. The effective width of the bridge opening,  $b$ , is planned to be 200 ft. The problem is to compute the backwater at cross section 1 caused by the constriction.

The distance to the approach cross section,  $L_w$ , is computed by determining the geometric constriction ratio from equation 11 and the  $L_w/b$  ratio from table 6.

$$m' = 1 - b/B \quad (11)$$

$$m' = 1 - \frac{200}{2000} = 0.90$$

From table 6 for  $m' = 0.90$ ,  $L_w/b = 2.78$ .

$$L_w = 2.78 \times 200 \text{ ft} = 556 \text{ ft}$$

The approach section was surveyed approximately 556 ft upstream from the bridge section 2. The result is shown in figure 15. In addition, a section along the highway centerline and a section approximately 200 ft downstream were surveyed. During the survey, the Manning's roughness coefficients,  $n$ , were selected for each cross section. Since the roughness was relatively uniformly distributed on the flood plain, an  $n = 0.14$  was selected for the flood plain for each cross section. In the main channel,  $n = 0.050$  for each cross section.

The following steps are generally required to compute backwater:

Step 1.--Compute the natural water surface profile from section 4 to section 1 using step-backwater.

Step 2.--Using the natural profile as a first estimate, compute the hydraulic and geometric variables required in the solution of the contracted profile. These include:

$C$  - Coefficient of discharge (Matthai, 1967)

$L$  - Length of bridge abutment in the direction of the flow (Matthai, 1967)

$m'$  - Channel-geometric constriction ratio. This value has been estimated to locate the approach. It will vary only slightly for the contracted and uncontracted water-surface profile.

$L_{av}$  - Average streamline length in the approach reach

$K_q^{av}$  - Portion of approach conveyance,  $K_1$ , corresponding to the bridge width,  $b$  (Matthai, 1967)

The cross-section properties which were computed separately can be obtained from table 13. The energy coefficient was computed as

Table 13.--Cross-section properties for section 1

Water surface elevation <sup>1</sup>	Subsection	Area, ft <sup>2</sup>	Conveyance, ft <sup>3</sup> /s	Alpha	Beta
15.0	L.B.	980	12,300	---	---
	M.C.	1,260	127,400	---	---
	R.B.	3,060	71,400	---	---
Total		<u>5,300</u>	<u>211,100</u>	<u>4.01</u>	<u>1.75</u>
15.2	L.B.	1,140	15,700	---	---
	M.C.	1,300	134,200	---	---
	R.B.	3,250	78,800	---	---
Total		<u>5,690</u>	<u>228,700</u>	<u>4.00</u>	<u>1.74</u>
15.4	L.B.	1,290	19,300	---	---
	M.C.	1,340	141,200	---	---
	R.B.	3,440	86,400	---	---
Total		<u>6,070</u>	<u>246,900</u>	<u>3.98</u>	<u>1.73</u>
16.0	L.B.	1,750	32,200	---	---
	M.C.	1,460	162,800	---	---
	R.B.	4,010	111,100	---	---
Total		<u>7,220</u>	<u>306,100</u>	<u>3.85</u>	<u>1.68</u>
16.2	L.B.	1,910	37,000	---	---
	M.C.	1,500	170,300	---	---
	R.B.	4,200	119,900	---	---
Total		<u>7,610</u>	<u>327,200</u>	<u>3.81</u>	<u>1.67</u>
16.4	L.B.	2,060	42,100	---	---
	M.C.	1,540	177,900	---	---
	R.B.	4,390	129,000	---	---
Total		<u>8,000</u>	<u>349,000</u>	<u>3.77</u>	<u>1.66</u>
Cross-section properties for section 3 without the constriction (natural section)					
14.6	L.B.	910	12,200	---	---
	M.C.	1,240	124,100	---	---
	R.B.	2,970	67,800	---	---
Total		<u>5,120</u>	<u>204,100</u>	<u>3.95</u>	<u>1.74</u>
14.8	L.B.	1,060	13,900	---	---
	M.C.	1,280	130,800	---	---
	R.B.	3,160	75,000	---	---
Total		<u>5,500</u>	<u>219,700</u>	<u>4.02</u>	<u>1.75</u>
15.0	L.B.	1,210	17,500	---	---
	M.C.	1,320	137,700	---	---
	R.B.	3,340	82,600	---	---
Total		<u>5,870</u>	<u>237,800</u>	<u>3.98</u>	<u>1.73</u>

<sup>1</sup>Main channel conveyance is equal to  $K_q$  in this example.

Table 13.--Continued

Water surface elevation	Subsection	Area, ft <sup>2</sup>	Conveyance, ft <sup>3</sup> /s	Alpha	Beta
Cross-section properties for sections 2 and 3 (constricted)					
14.2	M.C.	1,170	110,300	---	---
14.4	M.C.	1,210	116,600	---	---
14.6	M.C.	1,250	122,900	---	---
14.8	M.C.	1,290	129,400	---	---
15.0	M.C.	1,330	136,000	---	---
Cross-section properties for section 4					
14.2	L.B.	780	9,900	---	---
	M.C.	1,200	117,500	---	---
	R.B.	2,780	60,900	---	---
Total		<u>4,760</u>	<u>188,300</u>	<u>3.93</u>	<u>1.74</u>
14.4	L.B.	910	12,200	---	---
	M.C.	1,240	124,100	---	---
	R.B.	2,970	67,800	---	---
Total		<u>5,120</u>	<u>204,100</u>	<u>3.95</u>	<u>1.74</u>
14.6	L.B.	1,060	13,900	---	---
	M.C.	1,280	130,800	---	---
	R.B.	3,160	75,000	---	---
Total		<u>5,500</u>	<u>219,700</u>	<u>4.02</u>	<u>1.75</u>

$$\alpha = \frac{\sum k_i^3 / a_i^2}{(K^3 / A^2)}$$

and the momentum coefficient,  $\beta$

$$\beta = \frac{\sum k_i^2 / a_i}{K^2 / A}$$

where  $k_i$  is the subsection conveyance,  $a_i$  is the subsection area,  $K$  is the cross-section conveyance, and  $A$  is the cross-section area.

Step 3.--Using step backwater, compute the contracted water-surface profile from section 4 to section 1. The water-surface elevation at section 4 is assumed to be at the natural condition in the contracted case.

Step 4.--Recompute the variables in step 2.

Step 5.--Continue with steps 3 and 4 until the change in the recomputed variables is not significant and the desired accuracy is achieved.

Step 6.--Compute backwater at section 1 by subtracting the natural water-surface elevation from the contracted water-surface elevation.

Step 1. Compute the natural profile. The energy balance between section 3 and 4 is

$$h_{3n} + \alpha_{3n} \frac{Q^2}{2gA_3^2} = h_4 + \alpha_4 \frac{Q^2}{2gA_4^2} + h_{f(3-4)}$$

where

$$h_{f(3-4)} = \frac{bQ^2}{K_{3n} K_{4n}}$$

Assume the natural stage at section 3 is 14.7 ft and use the cross-section properties in table 13

$$h_{f(3-4)} = \frac{200 \times 6,400^2}{211,900 \times 211,900}$$

$$= 0.18 \text{ ft}$$

$$\alpha_4 \frac{Q^2}{2gA_4^2} = 3.99 \times \frac{6400^2}{64.3 \times 5310^2} = 0.09 \text{ ft}$$

$$\alpha_{3n} \frac{Q^2}{2gA_{3n}^2} = 3.99 \times \frac{6400^2}{64.4 \times 5310^2} = 0.09 \text{ ft}$$

$$h_{3n} + 0.09 = 14.5 + 0.09 + 0.18$$

$$h_{3n} = 14.68 \text{ ft}$$

$$\text{assumed } h_{3n} = 14.7 \text{ ft}$$

Therefore, the natural stage at section 3,  $h_{3n}$ , is 14.7 ft.

The distance from section 3 to section 1 is  $L + L_w = 40 + 556 = 596$  ft. The energy balance between sections 1 and 3 is

$$h_{1n} + \alpha_{1n} \frac{Q^2}{2gA_{1n}^2} = h_{3n} + \alpha_{3n} \frac{Q^2}{2gA_3^2} + h_{f(1-3)}$$

where

$$h_{f(1-3)} = \frac{(L + L_w) Q^2}{K_{1n} K_{3n}}$$

Assume the natural water-surface elevation at section 1 is 15.2 ft.

$$h_{f(1-3)} = \frac{596 \times 6400^2}{228,700 \times 211,900} = 0.50 \text{ ft}$$

$$\alpha_{3n} \frac{Q^2}{2gA_3^2} = 0.09 \text{ (previous computation)}$$

$$\alpha_{1n} \frac{Q^2}{2gA_{1n}^2} = 4.01 \times \frac{6400^2}{64.3 \times 5690^2} = 0.08 \text{ ft}$$

$$h_{1n} + 0.08 = 14.7 + 0.09 + 0.50$$

$$h_{1n} = 15.21 \text{ ft}$$

$$\text{Assumed } h_{1n} = 15.2 \text{ ft}$$

Therefore, the natural water-surface elevation at section 1 is 15.2 ft.

Step 2. The following variables are computed for the first trial computation of the contracted water-surface profile. For  $h_1 = h_{1n} = 15.2$  ft,  $K_1 = 134,200$   $\text{ft}^3/\text{s}$  and  $K_1 = 228,700 \text{ ft}^3/\text{s}$ . Since  $m = (1 - K_1^2/K_1^2)^{1/2}$ ,  $m = 0.41$ . In addition,

$L/b = 40/200 = 0.20$ . From Matthai (1967), find  $C = 0.76$ . From equations 25 and 26,  $\alpha_3 = 1.73$  and  $\beta_3 = 1.32$ . For  $L_w/b = 2.78$  and  $m' = 0.90$ ,  $L_{av}/b = 3.95$  from table 5. Therefore,

$$L_{av} = 3.95 \times 200 \text{ ft} = 790 \text{ ft}$$

Step 3. The step backwater equations are applied to the constricted flow. The energy balance between section 3 to 4 is

$$h_3 + \alpha_3 \frac{Q^2}{2gA_3^2} = h_4 + \alpha_4 \frac{Q^2}{2gA_4^2} + h_e + h_{f(3-4)}$$

where

$$h_{f(3-4)} = \frac{bQ^2}{K_c K_{4n}} \quad (23)$$

and

$$h_e = \frac{Q^2}{2gA_4^2} \left[ (2\beta_4 - \alpha_4) - 2\beta_3 \frac{A_4}{A_3} + \alpha_3 \left( \frac{A_4}{A_3} \right)^2 \right] \quad (24)$$

Assume the stage at section 3 is 14.60 ft. At this stage,  $K_3 = 122,900 \text{ ft}^3/\text{s}$  and from step 2,  $K_4 = 134,200 \text{ ft}^3/\text{s}$ . The smaller of  $K_3$  or  $K_4$  is the controlling conveyance in the following computations. In this case,  $K_c = K_3$ .

$$h_e = 0.44 \text{ ft}$$

$$h_{f(3-4)} = 0.31 \text{ ft}$$

$$\alpha_4 \frac{Q^2}{2gA_4^2} = 0.09 \text{ ft}$$

$$\alpha_3 \frac{Q^2}{2gA_3^2} = 0.71 \text{ ft}$$

$$h_3 + 0.71 = 14.5 + 0.09 + 0.44 + 0.31$$

$$h_3 = 14.6 \text{ ft}$$

$$\text{Assumed } h_3 = 14.6 \text{ ft}$$

Therefore, the contracted water-surface elevation at section 3 is 14.6 ft. The energy balance between section 1 and 3 is

$$h_1 + \alpha_1 \frac{Q^2}{2gA_1^2} = h_3 + \alpha_3 \frac{Q^2}{2gA_3^2} + h_{f(2-3)} + h_{f(1-2)}$$

where

$$h_{f(2-3)} = \frac{LQ^2}{K_3^2}$$

and

$$h_{f(1-2)} = \frac{L_{av}Q^2}{K_1K_C}$$

Assume the stage at section 1 is 16.2 ft. From step 3,  $K_3 = 122,900$  and from step 2,  $K_1 = 134,200 \text{ ft}^3/\text{s}$ . Since  $K_3$  is less than  $K_q$ ,  $K_C = K_3$ . Also from table 13,  $K_1 = 327,200 \text{ ft}^3/\text{s}$ .

$$h_{f(2-3)} = 0.11 \text{ ft}$$

$$h_{f(1-2)} = 0.80 \text{ ft}$$

$$\frac{\alpha_1 Q^2}{2gA_1^2} = 0.04 \text{ ft}$$

$$\frac{\alpha_3 Q^2}{2gA_3^2} = 0.71 \text{ ft (previous computation)}$$

$$h_1 + 0.04 = 14.6 + 0.71 + 0.11 + 0.80$$

$$h_1 = 16.18 \text{ ft}$$

$$\text{Assumed } h_1 = 16.2 \text{ ft}$$

Therefore, stage at section 1 is 16.2 ft.

Step 4. The variables in step 2 are recomputed. For  $h_1 = 16.2 \text{ ft}$ ,  $K_1 = 170,300 \text{ ft}^3/\text{s}$  and  $K_1 = 327,200 \text{ ft}^3/\text{s}$ . From Matthai (1967) for  $m = 0.48$  and  $L/b = 0.20$ ,  $C = 0.75$ . Therefore  $\alpha_3 = 1.78$  and  $\beta_3 = 1.33$ . None of the other variables change in this case.

Step 5. The small change in  $C$  affects the value of  $\alpha_3$  and  $\beta_3$ . In this case, the answers will not change at the level of significance being used. The conveyance,  $K_q$ , is still larger than  $K_3$  so that the controlling conveyance,  $K_C$ , is still  $K_3$ .

Step 6.--Backwater at section 1 is the difference between the contracted water surface and the natural water surface elevations.

$$\begin{aligned} \text{Contracted water surface elevation} &= 16.2 \text{ ft} \\ \text{Natural water surface elevation} &= \underline{15.2 \text{ ft}} \\ &\quad 1.0 \text{ ft} \end{aligned}$$

There were no spur dikes used in this example. Had there been, an additional computation would be needed to compute the stage at the toe of the dikes. The energy balance between section 3 and the toe of the dikes is:

$$h_d + \alpha_d \frac{Q^2}{2gA_d^2} = h_3 + \alpha_3 \frac{Q^2}{2gA_3^2} + h_f(2-3) + h_f$$

where

$$h_f(2-3) = \frac{LQ^2}{K_3^2}$$

and

$$h_f(d-2) = \frac{L_d Q^2}{K_3 K_d}$$

After finding  $h_d$ , balance the energy equation between sections 1 and d.

$$h_1 + \alpha_1 \frac{Q^2}{2gA_d^2} = h_d + \alpha_d \frac{Q^2}{2gA_d^2} + h_f$$

where

$$h_f(1-d) = \frac{L_{av} Q^2}{K_1 K_c}$$

In this case the controlling conveyance would be the smallest of  $K_d$ ,  $K_3$ , or  $K_q$ .

For purposes of this example, the approach section was located according to the criteria expressed by equation 18 or table 6. If the approach section is surveyed at another location, use the actual distance,  $L_w$ , to determine  $L_{av}$  from table 5.

#### REFERENCES

Benson, M. A., and Dalrymple, T., 1967, General field and office procedures for indirect discharge measurements: U. S. Geol. Survey Techniques Water-Resources Inv., book 3, chap. A1, 30 p.

Bradley, J. N., 1960, Hydraulics of bridge waterways: Bur. Public Roads, Hydraulic Design Ser. No. 1, 53 p.

1970, Hydraulics of bridge waterways: Federal Highway Admin., Hydraulics Design Ser. No. 1, 111 p.

Chow, V. T., 1959, Open-channel hydraulics, New York, McGraw-Hill, Inc., 680 p.

Churchill, R. V., Brown, J. W., and Verhey, R. F., 1948, Complex variables and applications, New York, McGraw-Hill, Inc., 332 p.

Cragwall, J. S., Jr., 1958, Computation of backwater at open-channel constrictions: U. S. Geol. Survey open-file rept., 23 p.

Franques, J. T., and Yannitell, D. W., 1974, Two-dimensional analysis of backwater at bridges: Proc. Am. Soc. Civil Engs., Jour. of the Hydraulics Div., v. 100, no. HY3, p. 379-392.

Henderson, F. M., 1966, Open channel flow, New York, The MacMillan Co., 522 p.

Hulsing, H., 1967, Measurement of peak discharge at dams by indirect method: U. S. Geol. Survey Techniques Water-Resources Inv., book 3, chap. A5, 29 p.

Kindsvater, C. E., and Carter, R. W., 1955, Tranquil flow through open-channel constrictions: Am. Soc. Civil Engs. Trans., v. 120, p. 955-980.

Kindsvater, C. E., Carter, R. W., and Tracy, H. J., 1953, Computation of peak discharge at contractions: U. S. Geol. Survey Circ. 284, 35 p.

Laursen, E. M., 1970, Bridge backwater in wide valleys: Proc. Am. Soc. Civil Engs., Jour. of the Hydraulics Div., v. 96, no. HY4, p. 1019-1038.

Lui, H. K., Bradley, J. N., and Plate, E. J., 1957, Backwater effects of piers and abutments: Civil Eng. Dept., Colorado State Univ. Rept. CER57HKL10, 364 p..

Matthai, H. F., 1967, Measurement of peak discharge at width contractions by indirect methods: U. S. Geol. Survey Techniques Water-Resources Inv., book 3, chap. A4, 44 p.

Su, M. Y., 1973, Complex potential flow through a symmetric two-dimensional constriction: General Electric Company, NSTL, Tech. Rept. 73-51, 27 p.

Tracy, H. J., and Carter, R. W., 1955, Backwater effects of open-channel constrictions: Am. Soc. Civil Engs. Trans., v. 120, p. 993-1006.

USGS LIBRARY-RESTON



3 1818 00018985 0